ELSEVIER

Chemical Geology 235 (2006) 138–160

CHEMICAL GEOLOGY
INCLUDING
ISOTOPE GEOSCIENCE

www.elsevier.com/locate/chemgeo

High-field-strength elements in carbonatitic rocks: Geochemistry, crystal chemistry and significance for constraining the sources of carbonatites

Anton R. Chakhmouradian *

Department of Geological Sciences, University of Manitoba, 125 Dysart Road, Winnipeg, Manitoba, Canada R3T 2N2

Received 14 July 2004; received in revised form 5 June 2006; accepted 27 June 2006

Editor: S.L. Goldstein

Abstract

Carbonatites and related rocks exhibit a significant variation in their content of high-field-strength elements (HFSE), i.e. Ti, Nb, Ta, Zr and Hf. The average abundances of these elements (calculated for 119 localities worldwide) decrease from phoscorites and silicocarbonatites to calciocarbonatites to magnesiocarbonatites. The analytical data currently available for ferrocarbonatites are insufficient to establish if this trend persists through the entire carbonatitic series. In comparison with the primitive mantle, the average carbonatite has significantly higher Nb/Ta and Zr/Hf ratios, and lower Zr/Nb and Zr/Ta ratios (35, 60, 1 and 29, respectively). Alkali-ultramafic rocks associated with carbonatites exhibit, on average, higher Zr/Nb ratios and no (or little) depletion in heavy HFSE (Ta and Hf). Implications of these data for constraining the source(s) of intracratonic carbonatites are discussed using the Kola Alkaline Province (NW Russia and Finland) as an example. The bulk of incompatible HFSE (>85%) is estimated to reside in Ti, Nb and Zr oxide minerals (in particular, perovskite, pyrochlore, ilmenite, baddeleyite and zirconolite) and zircon, whereas a significant proportion of Ti is contained in magnetite and ferromagnesian silicates. The lowest recorded Nb/Ta and Zr/Hf ratios in the primary HFSE oxides and titanite (but not zircon) are significantly below the primitive-mantle values, which makes these phases an effective vehicle of heavy-HFSE fractionation at crustal levels. The HFSE geochemistry of carbonatites en masse is not consistent with their derivation from a hypothetical carbonate-rich alkali-ultramafic (e.g., nephelinitic) magma by either liquid immiscibility or crystal fractionation. The bulk of carbonatites are interpreted to originate by low-degree partial melting of a metasomatized $HFSE^{5+}$-enriched mantle source with elevated Nb/Ta and Zr/Hf ratios. The trace-element signature of carbonatites cannot be adequately explained by clinopyroxene-controlled decoupling of $HFSE^{5+}$ and $HFSE^{4+}$ during partial melting, and requires the presence of amphibole and, possibly, refractory phlogopite in their mantle source. The HFSE geochemistry, field relations and relative timing of Kola carbonatites and associated silicate rocks are consistent with their derivation by low-degree melting of a vertically heterogeneous amphibole-bearing mantle reservoir, followed by differentiation of the primitive magmas. The previously established volume, tectonic and geochemical constraints suggest that the metasomatic enrichment of the mantle may have resulted from reaction of garnet lherzolite with carbonate melts of asthenospheric provenance, which is in agreement with the published experimental and mantle-xenolith studies. There is no evidence for the presence of refractory rutile (i.e., subducted crust) in the postulated mantle source.

Keywords: High-field-strength elements; Carbonatites; Phoscorites; Silicocarbonatites; Fractionation; Liquid immiscibility; Mantle metasomatism; Kola Alkaline Province

* Fax: +1 204 474 7623.
E-mail address: chakhmou@ms.umanitoba.ca.

0009-2541/$ - see front matter © 2006 Elsevier B.V. All rights reserved.
doi:10.1016/j.chemgeo.2006.06.008

1. Introduction

High-field-strength elements (HFSE) are tetravalent and pentavalent transition metals that show broadly similar behavior in various geochemical processes owing to their high valence, relatively small and similar ionic radii, and intermediate electronegativity values (Appendix A). However, their significantly different thermodynamic properties, even within the geochemical "twin pairs" (Nb–Ta and Zr–Hf), undoubtedly affect bonding, speciation and fractionation of HFSE in magmas and hydrothermal fluids. About 80 minerals containing essential HFSE (Ti, Nb, Ta, Zr or Hf) have been described from carbonatites and related rocks to date. The principal HFSE carriers in carbonatites and phoscorites (i.e. oxide-phosphate-silicate-rich rocks of carbonatitic affinity) are complex oxide minerals belonging to the perovskite and ilmenite groups and anion-deficient derivatives from the fluorite structure type (see Table 1 for formulae). In some cases, these minerals form industrially viable concentrations of Nb (e.g., Niobec pyrochlore deposit in Canada: Gendron et al., 1984) and Zr (e.g., Kovdor baddeleyite deposit in Russia: Ivanyuk et al., 2002; Krasnova et al., 2004). Various aspects of the mineralogy of HFSE in carbonatitic rocks the Kola Alkaline Province have

Table 1
Major HFSE carriers in carbonatitic rocks: Compositional variation (wt.%) and key element ratios

Mineral group	TiO_2	Nb_2O_5	Ta_2O_5	Nb/Ta	ZrO_2	HfO_2	Zr/Hf
Mineral species	Mean (*n*)	Mean (*n*)	Mean (*n*)		Mean (*n*)	Mean (*n*)	
Formula	Range e.s.d.	Range e.s.d.	Range e.s.d.		Range e.s.d.	Range e.s.d.	
Ilmenite group:							
Ilmenite/pyrophanite	51.38 (44)	2.64 (44)	0.12 (27)	≥2.9 [a]	0.03 (20)	b.d	–
(Fe, Mn, Mg) (Ti, Nb, Fe^{3+}) O_3	46.20–58.80	0–8.50	0–0.57[a]		0–0.17 [b]		
	3.50	2.51	0.15		0.03		
Perovskite group:							
Primary perovskite/latrappite	42.55 (111)	10.49 (147)	0.53 (123)	≥1.8	0.60 (87)	0.04 (20)	≥3.3
(Ca, Na, REE) (Ti, Nb, Fe^{3+}) O_3	8.89–58.76	0–50.35	0–4.20		0–3.27 [c]	0–0.31	
	12.74	12.70	0.68		0.83	0.09	
Lueshite	4.08 (24)	73.35 (24)	0.83 (24)	≥11.2	0.25 (14)	b.d	–
(Na, Ca, REE) (Nb, Ti) O_3	1.09–12.78	57.30–78.21	0–5.18		0–0.85		
	2.38	4.63	1.40		0.30		
Deuteric perovskites [d]	40.21 (28)	12.62 (28)	0.45 (21)	≥2.5 [e]	0.07 (9)	b.d	–
(Ca, Na, REE) (Ti, Nb, Fe^{3+}) O_3	26.62–50.87	0.78–30.56	0–1.51[e]		0–0.12		
	6.10	9.15	0.42		0.04		
Pyrochlore group:							
Betafite/U-rich pyrochlore [f]	6.42 (138)	43.27 (141)	7.92 (141)	≥1.0	1.92 (91)	0.10 (9)	≥14.5
$(U, Ca)_{2-x}(Nb, Ta, Ti, Zr)_2 O_6(OH)_{1-y}\cdot nH_2O$	0.44–16.87	25.84–64.29	0–25.60		0–10.25	0–0.26	
	3.29	7.55	5.90		2.29	0.10	
Pyrochlore[f]	3.83 (121)	62.11 (123)	0.85 (117)	≥6.1	0.94 (99)	b.d	–
$(Ca, Na)_{2-x}(Nb, Ti)_2O_6(OH)_{1-y}\cdot nH_2O$	0.09–9.30	40.55–78.46	0–8.26		0–6.53		
	1.95	6.40	1.30		1.19		
Late-stage pyrochlores [g]	3.63(98)	66.58 (100)	1.11 (95)	≥2.0	0.46 (88)	b.d	–
$(Sr, Ba, REE, K, Pb, Th, Ca)_{2-x}$	0.03–11.98	30.97–86.78	0–13.08		0–8.68		
$(Nb, Ta, Ti, Zr)_2O_6(OH)_{1-y}\cdot nH_2O$	1.58	11.44	2.66		1.16		
Baddeleyite	0.11 (130)	0.65 (131)	0.22 (114)	≥0	97.12 (125)	1.68 (128)	≥17.0
ZrO_2	0–1.12 [h]	0–6.58	0–1.18		87.57–99.73	0.60–4.78	
	0.18	0.91	0.22		1.67	0.58	
Zirconolite/zirkelite	24.78 (181)	10.59 (181)	1.63 (169)	≥0.6	31.30 (181)	0.53 (168)	≥18.1
$(Ca, REE)Zr(Ti, Nb, Fe)_2O_7$	13.56–38.99	0.19–24.66	0–5.83		24.46–37.38	0–1.29	
	5.40	5.93	1.28		2.50	0.19	
Calzirtite	14.78 (26)	2.95 (26)	0.27 (20)	≥2.6	67.71 (26)	0.73 (21)	≥30.0
$Ca_2Zr_5Ti_2O_{16}$	10.50–17.94	0–8.50	0–0.80		64.79–70.12	0.21–1.95	

(continued on next page)

Table 1 (*continued*)

Mineral group	TiO_2	Nb_2O_5	Ta_2O_5	Nb/Ta	ZrO_2	HfO_2	Zr/Hf
Mineral species	Mean (*n*)	Mean (*n*)	Mean (*n*)		Mean (*n*)	Mean (*n*)	
Formula	Range e.s.d.	Range e.s.d.	Range e.s.d.		Range e.s.d.	Range e.s.d.	
	2.07	2.05	0.28		1.18	0.43	
Zircon group:							
Zircon	0.04 (17)	0.12 (18)	0.07 (10)	≥0	64.99 (43)	1.04 (40)	≥32.6
$ZrSiO_4$	0–0.29	0–0.80	0–0.26		59.65–67.18	0.04–1.74	
	0.08	0.27	0.08		1.60	0.38	
Garnet group:							
Titaniferous calcic garnets [i]	11.84 (41)	0.15 (37)	b.d	–	6.76 (41)	0.05 (6)	≥30.6
$Ca_3(Fe, Ti, Zr, Mg)_2(Si, Fe, Al)_3O_{12}$	5.23–17.12	0–0.48			1.34–29.24	0–0.32	
	3.35	0.17			5.56	0.13	
Cuspidine group:							
Wöhlerite/marianoite/niocalite	(48)[j]	(53)[j]	(41)[j]	≥17.6	(48)[j]	(41)[j]	≥31.2
$Na_{0-1}Ca_{2-7}(Zr, Nb)_{1-2}(Si_4O_{14})(O, OH, F)_4$	0.06–1.82	0.65–17.20	0–0.79		0.23–16.15	0–0.32	
Titanite group:							
Primary titanite	35.55 (28)	1.78 (28)	0.05 (16)	≥6.2	1.32 (28)	0.04 (16)	≥9.3
$Ca(Ti, Zr, Nb, Fe)SiO_4(O, OH)$	30.05–39.15	0–4.81	0–0.22		0–6.96	0–0.26	
	2.40	1.31	0.07		1.76	0.07	
Deuteric titanite	32.31 (68)	1.45 (68)	0.08 (8)	≥3.9	2.41 (68)	0.26 (19)	≥3.2
$Ca(Ti,Zr,Nb,Fe,Al)SiO_4(O,OH)$	22.61–40.05	0–11.37	0–0.47		0–15.31	0–0.46	
	4.41	2.44	0.17		4.19	0.17	

Elements, for which fewer than 5 analyses are available, are reported as b.d, i.e. below the limit of detection.

[a] A single analysis of ilmenite from Jacupiranga, Brazil, gave 1.2 wt.% Ta_2O_5 and Nb/Ta=0.7 (Gaspar and Wyllie, 1983); this value was not included in the calculation of the mean Ta_2O_5 content; Garanin et al. (1980) obtained a similar mean Ta_2O_5 value (0.1 wt.%), but a lower Nb_2O_5 value (1.1 wt.%) for ilmenite from carbonatites (i.e. Nb/Ta_{mean}=9.4).

[b] A single analysis of ilmenite from Prairie Lake, Canada, gave 0.5 wt.% ZrO_2 (Chakhmouradian and Mitchell, unpubl. data); this value was not included in the calculation of the mean ZrO_2 content.

[c] Pozharitskaya and Samoylov (1972) reported up to 6.1 wt.% ZrO_2 in perovskite from Gornoozerskiy (Ozernyi) complex, Siberia, but these data were not confirmed by electron-microprobe analysis (EMPA) (author's unpubl. work); Pozharitskaya and Samoylov's high-Zr data were not included in the calculation of the mean ZrO_2 content.

[d] This category includes a variety of Na, REE and/or Nb-enriched perovskite-group minerals that form overgrowths on primary perovskite under hydrothermal conditions, i.e. ceroan perovskite, loparite-(Ce) and ceroan calcian lueshite.

[e] A single analysis of loparite-(Ce) from Afrikanda, Kola, gave 1.6 wt.% Ta_2O_5 at 0.8 wt.% Nb_2O_5, i.e. Nb/Ta=0.4 (Chakhmouradian and Zaitsev, 1999); this value was not included in the calculation of the mean Ta_2O_5 content.

[f] A division between U-rich and "normal" pyrochlore is arbitrarily set at 2.0 wt.% UO_2 (cf. Subbotin and Subbotina, 2000).

[g] This category includes a variety of cation-and anion-deficient pyrochlore-group minerals that typically replace primary pyrochlores under hydrothermal and surface conditions, i.e. strontiopyrochlore, bariopyrochlore, ceriopyrochlore-(Ce), kalipyrochlore, plumbopyrochlore and "thoriopyrochlore".

[h] A single analysis of baddeleyite from Afrikanda, Kola, gave 2.1 wt.% TiO_2 (Chakhmouradian and Zaitsev, 1999); this value was not included in the calculation of the mean TiO_2 content.

[i] This category includes primary garnets compositionally intermediate with respect to andradite, schorlomite, kimzeyite and morimotoite; deuteric Al-rich "hydrogarnets" (hibschite and its Ti- or Fe-rich counterparts) are not included in this dataset.

[j] Mean values were not calculated because there is no continuous compositional variation among the three cuspidine-group minerals found in carbonatites.

been recently summarized by Chakhmouradian and Williams (2004). These authors have remarked on several unusual compositional characteristics of HFSE minerals from carbonatitic rocks, such as large and systematic variations in Zr/Hf and Nb/Ta ratios among the different groups of minerals and successive generations of the same mineral. It is impossible to relate these features to the whole-rock geochemistry of carbonatites, to the composition of their putative mantle source, or even to the evolution of carbonatite melts/fluids using the data available in the literature, because the most recent review of carbonatite geochemistry (Woolley and Kempe, 1989) is based on a limited dataset and lacks reliable data for Ta and Hf. Accordingly, the objectives of the present work were to revisit the distribution of HFSE in carbonatitic rocks, and to link these

geochemical data to the origin and early evolutionary history of their parental melts. The Kola Alkaline Province of northwestern Russia and northern Finland (hereafter, Kola) was chosen for the discussion of carbonatite petrogenesis, because this is unquestionably one of the best-studied areas of carbonatite magmatism in the world. Here, carbonatites occur in an extensional intracratonic environment, predominantly in association with silica-undersaturated alkaline rocks (Bulakh et al., 2004), i.e. in the setting characteristic of most carbonatites worldwide.

2. Geochemistry of HFSE in carbonatitic rocks

2.1. General comments

Carbonatitic rocks exhibit extreme variability in their HFSE contents. The absolute abundances of these elements can vary by two orders of magnitude within the same petrographic unit, even for extrusive/hypabyssal rocks lacking cumulus HFSE phases (e.g., Viladkar and Wimmenauer, 1986, their Table 10). Thus, it would be an oversimplification to claim enrichment of any of the HFSE as a distinct geochemical signature of *all* carbonatites or phoscorites (Table 2). In fact, the most notable feature of HFSE distribution in carbonatites, and one that has not been previously recognized, is a conspicuously non-normal distribution of data on a histogram (Fig. 1). More than 63% of all analyses compiled in the present work (Appendix B) have under 0.15 wt.% TiO_2, 200 ppm Nb and 150 ppm Zr; in all cases, the median is significantly lower than the calculated average abundances of these elements (see below). From this observation, it follows that element ratios (such as Nb/Ta or Zr/Nb) may be more informative for backtracking the evolution of carbonatitic magmas and fluids than the ppm values.

Another worthwhile comment stems from the statistics on the geographic distribution of carbonatites included in the present survey (Appendix B). Taking into account that the overwhelming majority of reports on the geology of carbonatites published in the past 17 years contain whole-rock trace-element data, these statistics can serve as a measure of how well a specific area of alkaline magmatism is studied. The best geochemically characterized are the European and African carbonatites, for which the number of "published" localities per 1×10^6 km^2 is 2.4 and 1.5, respectively, i.e. significantly higher than the world average of 0.9. The least studied are Australian carbonatites, where that number is only 0.2 localities per 1×10^6 km^2. Thus, the dataset discussed below is somewhat geographically biased (Fig. 2).

Table 2
High-field strength elements: relative abundances

TiO2 (wt.%)	Nb (ppm)	Ta (ppm)	Zr (ppm)	Hf (ppm)
mean (*n*)	mean (*n*)	mean (*n*)	mean (*n*)	mean (*n*)
range	range	range	range	range
e.s.d.	e.s.d.	e.s.d.	e.s.d.	e.s.d.
Phoscorites and silicocarbonatites (non-discriminated)				
1.83 (48)	557.2 (41)	32.0 (26)	729.1 (44)	12.8 (25)
0.03–7.71	12–12237	0–280	16–5410	0–66.4
1.40	1531.4	64.8	967.0	14.2
Calciocarbonatites				
0.28 (116)	343.1 (105)	9.1 (65)	281.4 (113)	4.9 (60)
0–2.40	0–6174	0–102	0–2867	0–33.6
0.38	697.6	17.9	428.3	7.3
Magnesiocarbonatites				
0.23 (50)	255.4 (45)	8.1 (28)	248.4 (51)	4.1 (26)
0–1.94	0–2200	0–60	0–3172	0–71.3
0.36	405.8	12.3	339.1	7.6
Ferrocarbonatites				
0.33 (23)	252.4 (21)	9.3 (11)	146.2 (22)	1.6 (9)
0–1.61	5–1980	0–41.5	0–1050	0–9.0
0.49	373.9	14.7	199.2	1.6
All carbonatites (averages of calcio-, magnesio- and ferrocarbonatites)				
0.28 (189)	308.9 (171)	8.9 (104)	256.4 (186)	4.3 (95)
0–2.40	0–12237	0–280.0	0–5410	0–71.3
0.39	598.9	16.1	385.3	7.1
	Nb/Ta=34.9		Zr/Hf=59.6	
Carbonatites associated with alkali-ultramafic rocks (Samoylov, 1984)				
0.30 (800)	290 (790)	13.0 (740)	320 (790)	1.9 (746)
0.03–1.73	7–2790	0–422	5–1260	0–8.4
	Nb/Ta=22.3		Zr/Hf=168.4	
Alkali-ultramafic intrusions, Kola (Arzamastsev et al., 2001)				
2.68	95.8	5.5	347.0	7.6
	Nb/Ta=17.4		Zr/Hf=45.7	
Continental crust (Wedepohl, 1995)				
0.86	19	1.1	203	4.9

This survey was compiled using whole-rock analyses from 72 post-1988 studies, not including the data of Woolley and Kempe (1989, their Table 1.1), nor any of the earlier reviews on the geochemistry of carbonatites. The complete data set, list of localities and references are given in Appendix B. Note that although the estimates of Samoylov (1984) are based on a large number of analyses, they represent a very limited number of localities.

2.2. HFSE distribution in carbonatitic rocks: numbers and trends

The summary of HFSE distribution in carbonatitic rocks is presented in Table 2, which was compiled following the approach of Woolley and Kempe (1989), i.e.

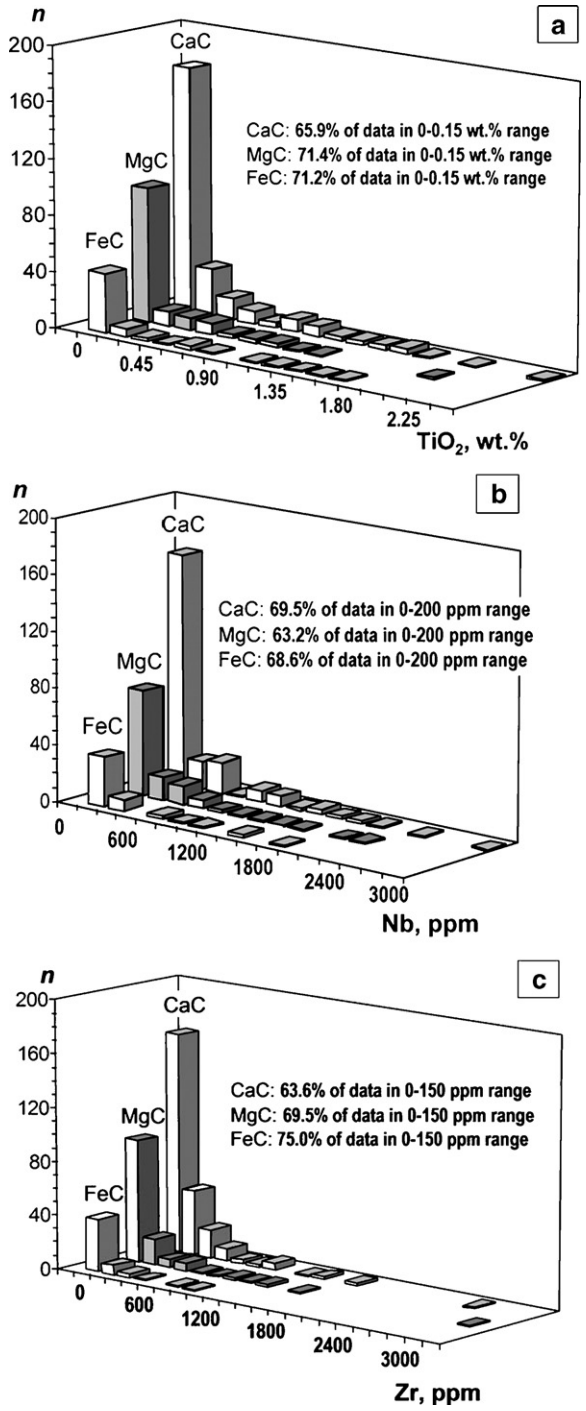

Fig. 1. Histograms of (a) Ti, (b) Nb and (c) Zr distribution in the three major types of carbonatites for the complete analytical dataset included in Appendix B.

multiple analyses for a single carbonatite body (or facies) were averaged, and these values then used to calculate the overall averages to avoid "overrepresentation" of a specific carbonatite locality (see also Appendix B). Unlike in the previous compilations, the average HFSE abundances for phosphate- and silica-rich rocks of carbonatitic affinity (i.e. phoscorites and silicocarbonatites) were also calculated. Although the latter category comprises rocks of very diverse modal composition, it was not subdivided because there is no appropriate, universally adopted nomenclature for these rocks. The geochemically distinct Sr–Ba-rich and HFSE-poor carbonate rocks, associated with potassic alkaline lithologies (e.g., Mushugai-Khuduk in Mongolia, Murun and Khalyuta in eastern Siberia: Dorfman and Kapustin, 1991; Entin et al., 1991; Bulnaev, 1996), was not included in this dataset, as their petrological status remains uncertain (Borisov, 1985; Vorob'ev, 2000). In total, ca. 580 recently published whole-rock analyses and author's own unpublished data, representing 119 localities of intrusive and extrusive carbonatitic rocks worldwide (including 8 Paleozoic complexes at Kola) were used in this survey. Because the available Ta and Hf data for the Kola localities are extremely limited, it was assumed that the trace-element budget of the Kola carbonatites (or, at least, the proportion among individual HFSE) does not deviate much from that of carbonatites en masse. This assumption is probably valid, considering the identical (to the first decimal place) Zr/Nb ratios in the Kola and global data sets.

Of particular relevance to the present work is the abundance of Nb and Zr in carbonatitic parageneses. Although Nb enrichment has been conventionally considered an important geochemical signature of these rocks, there are many examples of carbonatites whose Nb contents are near or below the detection limit of neutron-activation, inductively-coupled plasma mass-spectrometry, or other methods conventionally employed for that type of analytical work (e.g., Dunworth and Bell, 2001). There are even cases where carbonatites have lower Nb contents than their surrounding carbonate wallrocks (e.g., Le Bas et al., 1992). Analysis of the recently published literature shows that Nb contents in

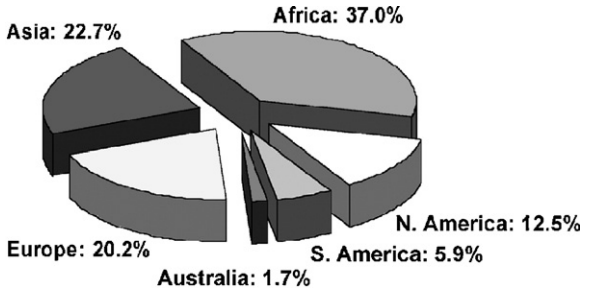

Fig. 2. Geographic distribution of carbonatite localities included in Table 2 and Appendix B.

the 600–2000 ppm range, i.e. the carbonatite averages of Gold (1963) and Woolley and Kempe (1989), are an exception rather than the norm (Table 2, Fig. 1). In contrast, our Zr averages are consistently higher for magnesiocarbonatites and calciocarbonatites than the values quoted in the latter study (130–190 ppm), but lower than Gold's (1963) estimate. However, there are also numerous examples of Zr-poor carbonatites, some of which contain less Zr than their metasomatised country rocks (e.g., Bagdasarov, 1993).

Phoscorites and silicocarbonatites are significantly enriched in all HFSE in comparison with bona fide carbonatites; the abundances of these elements also decrease from calciocarbonatites to magnesiocarbonatites. There is also a further decrease in Zr and Hf contents toward ferrocarbonatites, not accompanied by any significant change in Nb amount, whereas the Ti and Ta abundances actually increase (Table 2). However, it is premature to seek an explanation for the "anomalous" behavior of HFSE in ferrocarbonatites, given the limited amount of trace-element data available for these rocks in the literature (11 analyses reporting both Ta and Hf). Further geochemical studies of ferrocarbonatites (especially those considered primary, rather than metasomatic, rocks) are clearly required to establish if the trend of decreasing HFSE persists in Fe-rich members of the carbonatitic series.

With the exception of higher Hf (and, thus, lower Zr/Hf), the HFSE contents averaged for all carbonatites included in this survey are close to the estimates of Samoylov (1984) (Table 2). The significant discrepancy in Hf content probably arises from the fact that analytical methods employed in the earlier studies provided less accurate results at low-ppm levels. This explanation is consistent with much higher Zr/Hf ratios (202–240) determined for the Kovdor and Turiy Mys carbonatites by Samoylov (1984) in comparison with the more recent data of Ivanikov et al. (1998) and Verhulst et al. (2000) for the same rocks, which give Zr/Hf=36–72. Samoylov's estimate is clearly erroneous because it would require unrealistic degrees of Hf fractionation relative to the composition of the silicate Earth (Zr/Hf=37; McDonough and Sun, 1995). Assuming that the average composition of carbonatites worldwide typifies that of the Kola carbonatites, the latter are significantly enriched in Nb and Ta, strongly depleted in Ti, and have somewhat lower levels of Zr and Hf relative to the associated alkali-ultramafic lithologies (Arzamastsev et al., 2001). This has important implications for the discussion of carbonatite petrogenesis, which will be addressed in Section 4 below. Relative to the average composition of continental crust (Wedepohl, 1995), carbonatites en masse are strongly enriched in Nb and Ta, moderately enriched in Zr (but not Hf), and depleted in Ti.

3. HFSE hosts in carbonatitic rocks

3.1. Crystal-chemical controls

Partitioning of HFSE among crystallographic sites of different geometry and, hence, their incorporation in different crystal structures is controlled by charge constraints and small, but appreciable differences in ionic radii (Appendix A). To date, only Ti^{4+} (the smallest HFSE cation) has been shown conclusively to substitute in the tetrahedrally coordinated sites in the structure of some mafic silicates (e.g., Oberti et al., 1992), although analogous data for carbonatitic minerals are lacking. A detailed examination of titaniferous garnets from the Afrikanda silicocarbonatite at Kola (Chakhmouradian and McCammon, 2005; Chakhmouradian et al., 2005) found no evidence for $^{[4]}Ti^{4+}$ in these minerals (cf. Scordari et al., 1999). Ti^{4+} in a square-pyramid five-fold coordination occurs in some alkali titanosilicates (e.g., lamprophyllite: Krivovichev et al., 2003), which are relatively common in peralkaline silicate rocks but exceedingly rare in carbonatites (e.g., Kjarsgaard and Peterson, 1991). Appreciable quantities of these titanosilicates may be expected in fenitic aureoles surrounding some plutonic carbonatites, or in metasomatic "carbonatites" developed after alkaline silicate rocks (such as foidolites or fenites). $^{[5]}Ti^{4+}$ in an unusual, trigonal-bipyramidal environment occurs in zirconolite, a common Zr phase in carbonatites and phoscorites (Table 1). Neither Nb nor Zr was detected at this site by single-crystal structure refinement (Sinclair and Eggleton, 1982). The most typical coordination environment for Ti^{4+}, Nb^{5+} and Ta^{5+} is octahedra showing various degrees of distortion and cation-oxygen distances in the range 1.8–2.1 Å. The substitution of Nb or Ta for Ti is constrained not only by the availability of pentavalent HFSE, but also by the flexibility of the host structure, because such substitution would require incorporation of lower-charged cations (or formation of vacancies) in proximal crystallographic sites. The most common coupled substitutions are $NaNbCa_{-1}Ti_{-1}$ (e.g., perovskite group: Kukharenko et al., 1965; Kapustin, 1986), $CaNbREE_{-1}Ti_{-1}$ (e.g., zirconolite: Giere et al., 1998), and $NbFe^{3+}Ti_{-2}$ (zirconolite, perovskite and titanite: ibid., Chakhmouradian, 2004). In most cases, the "ancillary" substituent cations (i.e. Na^{+}, Ca^{2+} or Fe^{3+}) are readily available in the melt/fluid, which explains a significant extent of Nb substitution in Ti minerals from carbonatites (Table 1).

Zr^{4+} and Hf^{4+} are larger than the other HFSE cations (Appendix A) and show clear preference for a higher coordination, typically seven- or eight-fold (baddeleyite and zircon, respectively), with mean Zr–O distances of

ca. 2.2 Å. The structure of calzirtite comprises both ZrO_7 and ZrO_8 polyhedra (Sinclair et al., 1986). The amount of Zr substituting for Ti in octahedrally-coordinated positions is typically limited. Extensive Zr-for-Ti substitution requires that cations in adjacent crystallographic sites are also replaced with comparatively larger cations to minimize a mismatch between the coordination polyhedra and, thereby, stabilize the structure. For example, zirconian garnets typically contain an elevated proportion of Al replacing Si in the tetrahedrally coordinated sites (Armbruster et al., 1998). Obviously, this requirement places further constraints on the extent of Zr (and Hf) substitution in Ti phases. The above considerations explain why the Zr-for-Ti substitution in carbonatitic minerals is generally more restricted than the Nb-for-Ti substitution. For example, in primary ilmenite and perovskite-group minerals, the maximum recorded Nb/Ti ratios are one order of magnitude greater than the maximum Zr/Ti ratios (Appendix C). One exception is titanite, in which the two values are similar.

Although many inorganic compounds with $^{[6]}Ti^{4+}$ have a Zr-based structural analogue (e.g., perovskite and $CaZrO_3$), continuous solid solutions between Ti- and Zr-end-members do not exist among minerals. However, miscibility between the two end-members may be sufficient to cross the 50 mol% boundary required to define a new mineral species (e.g., Ti–Zr garnet series). Most major Ti and Nb phases in carbonatites are capable of accommodating at least several wt.% and, in some cases, in excess of 10 wt.% ZrO_2 (Table 1). Likewise, Zr minerals commonly contain Ti and Nb, whose relative proportion depends largely on the site geometry and, for Nb, tolerance of adjacent crystallographic sites for heterovalent substitutions. Structures with $^{[6]}Zr$ (Zr–O ca. 2.1 Å) and several cation sites of differing size (e.g., cuspidine-group minerals) are generally capable of accommodating more Nb or Ti than those with Zr in larger polyhedra and a limited capacity for coupled substitutions (such as baddeleyite or zircon). The maximum Nb/Zr ratios recorded in carbonatitic baddeleyite and zircon to date are <0.1 and, in 99% of analyses <0.05 (Appendix C).

3.2. Mineralogy of HFSE in carbonatitic rocks: major HFSE hosts

The compositional characteristics of major HFSE carriers in phoscorites and carbonatites are summarized in Table 1 which was compiled using 87 literature sources and author's unpublished data (in total, ca. 1180 entries); the complete dataset and references are given in Appendix C. Simple calculations show that even trace amounts of these minerals are sufficient to account for the average HFSE contents in carbonatitic rocks. For example, 250 ppm Zr corresponds to about 0.03 wt.% of baddeleyite or 0.05 wt.% zircon in the rock, whereas 300 ppm Nb to 0.06 wt.% of lueshite or 0.07 wt.% of Na–Ca pyrochlore. These numbers are comparable to or, in some cases, well below the actual concentrations of these minerals in carbonatitic rocks (Mariano, 1989; Chakhmouradian and Williams, 2004). Hence, the bulk of the HFSE is probably concentrated in accessory Ti, Nb and Zr oxides (especially baddeleyite, $CaZrTi_2O_7$ polymorphs, ilmenite-, perovskite-, and pyrochlore-group phases) and, in some cases, zircon. This conclusion is in agreement with Kapustin's (1986) estimate that oxide minerals account for >70% of the total Ti, Nb and Ta in carbonatites. The Ca-bearing HFSE silicates (garnets, cuspidine-group minerals and titanite) are of limited significance and essentially restricted to silicocarbonatites and late-stage (auto)metasomatic or hydrothermal parageneses.

From Table 1, the following important observations can be made:

(i) All major HFSE oxides and titanite may potentially serve as vehicles of heavy-HFSE (Ta+Hf) fractionation, as their lowest recorded Nb/Ta and Zr/Hf values are significantly smaller than the respective ratios for the average carbonatite (Table 2);
(ii) Early-crystallizing Nb minerals (e.g., liquidus perovskite and U-rich pyrochlore) have generally lower Nb/Ta ratios in comparison with their more evolved counterparts (e.g., lueshite and Na–Ca pyrochlore);
(iii) Early-crystallizing Zr oxides have lower Zr/Hf ratios in comparison with Zr-bearing silicate phases (with the exception of titanite).

A progressive increase in Nb/Ta or Zr/Hf ratio is also expressed in the core-to-rim zoning of some HFSE minerals (e.g., Williams, 1996; Chakhmouradian and Zaitsev, 2002). At present, these general trends cannot be confidently extrapolated to less-common HFSE phases, in which Ta and/or Hf are present in low concentrations (≤ 0.5 wt.% respective oxides), because the compositional data available for these minerals are scarce, and only a small fraction of these analyses report Ta_2O_5 and/or HfO_2 contents. Quantitative determination of Ta and Hf by energy-dispersive EMPA (especially in silicates) is difficult due to peak overlaps, and some of the data reported in the literature may, in fact, be prone to analytical error. Note also that low Nb/Ta and Zr/Hf ratios observed in some late-stage minerals (e.g., ion-deficient

pyrochlores and titanite) do not necessarily reflect a changing HFSE budget in the carbonatite, because these minerals commonly form by subsolidus re-equilibration of the primary paragenesis with deuteric or invading fluids (e.g., Ba–Sr-rich pyrochlore after U-rich pyrochlore, titanite after liquidus perovskite, etc.). Thus, their HFSE abundances are controlled by the composition of the precursor phase and by the differing mobility of Nb and Ta complexes in aqueous fluids (for further discussion, see Chakhmouradian and Williams, 2004).

3.3. Magnetite and mafic silicates as minor HFSE hosts

Magnetite may be a significant HFSE host phoscorites and silicocarbonatites, which typically contain an appreciable content of this mineral. It can accommodate up to 27 wt.% TiO_2 (Macdonald et al., 1993), most of which is probably bound in ilmenite lamellae ubiquitous in titaniferous magnetite (e.g., Krasnova et al., 2004). All other HFSE are incompatible with respect to magnetite, but $HFSE^{5+}$ less so than Zr and Hf (Table 3). There is considerable discrepancy among the limited published data on the trace-element chemistry of this mineral. According to the estimates of Kirnarskii and Polezhaeva (1975), magnetite from the Kola carbonatites and phoscorites contains 0.004–0.020 wt.% Nb_2O_5 and 0.002–0.010 wt.% Ta_2O_5, of which as much as 75% is accommodated in the crystal structure. Very similar values were reported for magnetite by Kapustin (1986): 0.017 wt.% Nb_2O_5 and 0.002 wt.% Ta_2O_5 (average for early and late carbonatites from 7 different complexes), and Krasnova et al. (2004, their Table 4.2). The latter authors also report 0.01 wt.% ZrO_2 in samples from Kovdor. A similar range of values ($\leq$0.03 wt.% Nb_2O_5, 0.01 wt.% Ta_2O_5 and 0.02 wt.% ZrO_2) was determined for magnetite from several localities around the globe by Bagdasarov (1989), who, however, concluded that the peak HFSE values were due to micro-inclusions of baddeleyite, pyrochlore and other HFSE phases irremovable with conventional sample-preparation techniques. Appreciably lower figures were obtained by Kukharenko et al. (1965, p. 318) for the Kola samples (<20 ppm Nb and 10 ppm Ta) and by Kravchenko and Bagdasarov (1987) for magnetite from the Maimecha-

Table 3
HFSE partitioning in minerals and hypothetical parental melts

	Element ratios				Data sources
	Nb/Ta	Zr/Hf	Zr/Nb	Zr/Ta	
Primitive mantle	18	37	16	284	McDonough and Sun (1995)
Alkali–ultramafic complexes (Kola)	17	46	3.6	63	Arzamastsev et al. (2001)
Olivine–melilite melanephelinite [a]	18	47	2.1	39	Ivanikov et al. (1998)
Carbonatites [b]	35	60	0.8	29	This work

D [c]	Ti	Nb	Ta	Zr	Hf	Data sources
$^{Carb/Sil}D$ (exp, ~0.9 kbar, 990 °C)	0.41	0.50	0.10	0.016	0.009	Veksler et al. (1998a,b)
$^{Cpx/L}D$ (exp)	0.658	0.014	0.026	0.238	0.595	Skulski et al. (1994)
$^{Ol/L}D$ (exp)	0.011	1.7×10^{-4}	1.8×10^{-5}	4.5×10^{-3}	3.7×10^{-3}	Zanetti et al. (2004)
$^{Prv/L}D$ (exp, emp)	15.9	1.78	3.71	0.14	0.29	Corgne and Wood (2005), Onuma et al. (1981)
$^{Mgt/L}D$ (exp)	12.88	0.116	0.121	0.031	0.096	Nielsen and Beard (2000)
$^{Ttn/L}D$ (exp)	12.48	5.71	64.17	2.57	4.69	Prowatke and Klemme (2005)
$^{Bad/L}D$ (exp)	1.4	1.8	9.0	198	140	Klemme and Meyer (2003)

Fractionation models	Abundances (ppm)					Details
	Ti	Nb	Ta	Zr	Hf	
model 1	1715	756	34	2701	41	42.3% Ol, 36.9% Cpx, 6.3% Mgt, 4.5% Prv, 10% melt
model 2	1674	294	12.7	1113	17.8	18.75% Ol, 45% Cpx, 7.5% Prv, 3.75% Mgt, 25% melt
model 3 (*best fit*)	1680	316	8.9	254	6.8	31.4% Ol, 35.3% Cpx, 7.9% Prv, 3.1% Mgt, 0.3% Ttn, 0.4% Bad, 21.6% melt

[a] Believed to closely correspond to the average composition of hypothetical magma parental with respect to the Kola alkali-ultramafic rocks and carbonatites (Kukharenko et al., 1965).

[b] These values correspond to the "average" carbonatite calculated for 119 localities worldwide (Table 2); Kola carbonatites have the same Zr/Nb ratio; their Nb/Ta, Zr/Hf and Zr/Ta ratios could not be determined with certainty owing to the paucity of reliable Ta and Hf data.

[c] Partition coefficients for carbonate melt (Carb) relative to alkaline silicate melt (Sil); calcic clinopyroxene (Cpx), olivine (Ol), magnetite (Mgt), perovskite (Prv), titanite (Ttn) and baddeleyite (Bad) relative to silica-undersaturated melt (L); exp=experimental data; emp=empirical data.

Kotuy carbonatite complexes (<30 ppm Nb and <40 ppm Zr). These data, obtained by bulk analytical techniques, are in marked contrast with the few available microbeam determinations, which show less than 2 ppm Nb and 3 ppm Zr in magnetite (e.g., Ionov and Harmer, 2002). The high Nb and Zr contents (up to 0.05 wt.% and 0.21 wt.% respective oxides) detected in some African samples by EMPA (Dawson et al., 1996) are probably an analytical artifact as they fall well outside the range established for magnetite with similar Ti contents, including the crystals synthesized in Nb- and Zr-partitioning experiments (Nielsen and Beard, 2000).

It is even more difficult to estimate what proportion of HFSE is accommodated in the rock-forming silicates because pertinent trace-element data are scarce and practically limited to "wet" chemical and flame-spectrometric analyses of bulk samples. Ti is compatible or mildly incompatible with respect to most mafic minerals (Table 3), and significant quantities of this element may be accommodated in amphiboles (up to 5.9 wt.% TiO_2 in arfvedsonite: Macdonald et al., 1993), Mg–Fe micas (up to 13.8 wt.% TiO_2 in phlogopite: Ibhi and Nachit, 2000), clinopyroxene (up to 2.3 wt.% TiO_2 in aegirine: Andersen, 1988) and humite-group phases (up to 4.0 wt.% TiO_2 in clinohumite: Krasnova et al., 2004). Olivine is of comparatively lesser importance because its structure is not as tolerant to the (Mg, Fe) ⇔ Ti substitution, although anomalously Ti-rich forsterite has been reported from Kovdor phoscorites, Kola (Ivanyuk et al., 2002, p. 223). Undoubtedly, these minerals also incorporate minor quantities of incompatible HFSE that substitute for Ti (i.e. Nb, Ta, Zr and Hf). The average Zr contents in clinopyroxenes and amphiboles from carbonatitic rocks of Afrikanda and Kovdor at Kola were estimated to range between 0.02 and 0.07 wt.% (ibid.). According to Kapustin (1986), the average Nb and Ta contents in phlogopite and clinopyroxene are broadly similar (ca. 0.005 and <0.0005 wt.% respective oxides), and do not vary much between the early and late carbonatites. With the exception of the Nb estimate for clinopyroxene, these data are in reasonable agreement with HFSE abundances in mafic silicates from various non-carbonatitic alkaline rocks determined by modern analytical techniques. The measured Nb content of calcic clinopyroxene is consistently below 10 ppm (e.g., Downes et al., 2004; Akinin et al., 2005; Plá Cid et al., 2005).

Given that the HFSE minerals listed in Table 1 are capable of incorporating two or more orders of magnitude more Nb, Ta, Zr and Hf than associated mafic silicates and magnetite (see also Table 3), the contribution of the latter to the incompatible-HFSE budget of carbonatitic rocks is, in most cases, negligible. A crude estimate for the Afrikanda silicocarbonatite (Chakhmouradian and Zaitsev, 2004) and Kovdor phoscorite (Verhulst et al., 2000; Krasnova et al., 2004) shows that that contribution is on the order of 5–15% of the whole-rock total (cf. Kapustin, 1986). Because the published trace-element data for the mafic silicates and magnetite from carbonatitic rocks are very limited and, in general, lack consistency, they have questionable value as indicators of magma (fluid) evolution or element-fractionation paths. Further studies of the rock-forming minerals using microbeam mass-spectrometry techniques are warranted.

4. Discussion

4.1. HFSE geochemistry of carbonatites in a petrogenetic context

The Kola Alkaline Province was chosen as a model for the discussion of carbonatite petrogenesis, because it represents the most typical tectonic-igneous setting of carbonatites worldwide. This Province is well characterized, extensive, and comprises a large variety of carbonatitic and spatially associated silicate (ultramafic and alkaline) rocks. The majority of these rocks were emplaced in the Late Devonian in extensional tectonic settings. Further details of their petrology, mineralogy and geochemistry can be found elsewhere (e.g., Wall and Zaitsev, 2004). A number of differing genetic interpretations have been offered for the Kola carbonatites in the literature, with opinions ranging from (auto)metasomatic reworking of antecedent alkali-ultramafic rocks (Kukharenko et al., 1965) to derivation of carbonatites and (certain types of) silicate rocks from a common parental magma by liquid immiscibility (Ivanikov et al., 1998) or crystal fractionation (Verhulst et al., 2000) to their independent origin from mantle-derived melts (Sindern et al., 2004). As expected, this diversity reflects the global evolution of thought on the origin of carbonatites (for review, see Lee and Wyllie, 1998a). Whatever model is chosen to explain the origin of carbonatites at Kola and beyond, it has to account not only for their association and temporal relationships with ultramafic and alkaline silicate rocks, but also for their unusual trace-element signature. Assuming that the composition of carbonatites en masse (or, at least, the proportions among individual HFSE) exemplifies that of the Kola carbonatites (see Section 2), these rocks are enriched in $HFSE^{5+}$ relative to $HFSE^{4+}$, and relatively depleted in heavy HFSE (Ta and Hf). The associated silicate rocks, on the other hand, have Nb/Ta and Zr/Hf

ratios close to those of the primitive mantle, whereas their Zr/Nb and Zr/Ta ratios are about 4.4 times lower than the primitive-mantle values (Table 3). A nearly two-fold increase in Nb/Ta in carbonatites relative to the alkali-ultramafic lithologies has been also documented by Kapustin (1986). Ibhi et al. (2002) report progressive depletion in heavy HFSE, coupled with a decrease in Zr/Nb, from olivine nephelinite to calcite carbonatite at Jbel Saghro, Morocco. A significant drop in Zr/Nb ratio from olivine/clinopyroxene nephelinites, or the calculated bulk of intrusive alkali-ultramafic rocks, to associated carbonatites is observed also at Oldoinyo Lengai in Tanzania (Bell and Simonetti, 1996; Zaitsev and Keller, in press), Okorusu in Namibia (Le Roex and Lanyon, 1998), Lower Sayan in Siberia (Bagdasarov and Pukarev, 1989) and several other localities, for which no adjunct Ta or Hf data are available in the literature.

Significant deviation of HFSE ratios from the primitive-mantle values is not unique to carbonatites. Two notable examples include oceanic-island basalts and evolved granites. In the literature, such deviations are explained in terms of crystal fractionation (Linnen and Keppler, 2002), element fractionation during partial melting (David et al., 2000), or metasomatism in the Earth's mantle (Kamber and Collerson, 2000) and crust (Dostal and Chatterjee, 2000). The following discussion will examine the contemporary views on the genesis and evolution of carbonatites in the framework of HFSE geochemistry.

4.2. Liquid immiscibility?

Arzamastsev et al. (2001) have estimated that the Devonian magmatism at Kola involved a colossal volume of the upper mantle (on the order of 3–5 mln km^3), and produced about 15 000 km^3 of diverse alkaline magmas. About one-quarter of that volume crystallized to alkali-ultramafic silicate rocks, and some 2% to carbonatites (ibid.). Note that these estimates are based on the distribution of various rock types within specific complexes and, hence, are independent of individual views on the origin of carbonatites and their relationships with coeval silicate rocks (or lack thereof).

Had the Kola carbonatites derived from a putative carbonated alkali-rich silicate parent (e.g., melanephelinite), $HFSE^{5+}$, but not $HFSE^{4+}$, must have preferentially partitioned into the carbonatitic melt through either liquid immiscibility or crystal fractionation. The former mechanism is not supported by the available experimental data showing that the immiscibility is limited to Mg–Fe-poor alkali-rich magmas (Lee and Wyllie, 1998a), and that *all* HFSE partition into the silicate melt (Petibon et al., 1998; Veksler et al., 1998a; Suk, 2001; our Table 3). It is also important that liquid immiscibility cannot account for the strongly decoupled Zr/Hf signature of carbonatites (Petibon et al., 1998). Although immiscibility remained a popular view on the origin of carbonatites through the 1980–90s (e.g., Peterson, 1989; Dorfman and Kapustin, 1991; Kjarsgaard and Peterson, 1991; Ivanikov et al., 1998), most of that work rests primarily on equivocal textural evidence. Globular and similar textures, commonly cited as evidence of immiscible separation, comprise compositions outside the carbonate–silicate immiscibility "dome" (Lee and Wyllie, 1998a). Whereas fractionation of mafic silicates can theoretically drive a putative parental magma (melanephelinitic or melilititic) to a Mg–Fe-poor alkali-rich derivative capable of liquid separation (ibid.), the composition of carbonate globules is difficult to reconcile with the available experimental data (Veksler et al., 1998b, their Table 5; Wyllie and Lee, 1998, p. 1891). In our opinion, the textural and mineralogical characteristics of such globules (ocelli), including their variegated modal mineralogy, low-Sr calcitic composition of carbonate (in the absence of calcite-strontianite exsolution), inward pattern of crystal growth and abundance of zeolites and other minerals atypical of bona fide carbonatites (Peterson, 1989; Kjarsgaard and Peterson, 1991), at the very least, require that alternative petrogenetic mechanisms (e.g., vesiculation) be considered.

Liquid immiscibility has also been invoked to explain the association of carbonatites with phoscorites at several of the Kola localities (Lapin and Vartiainen, 1983; Lee et al., 2004). The models proposed thus far failed to explain why the alleged immiscibility textures are restricted to a few rare varieties of phoscorite and are absent from their "conjugate" carbonatites. Also, there is no pertinent experimental data at present to either substantiate or dispute these models. Recognition of immiscibility in natural systems is not trivial (e.g., Wyllie and Lee, 1998), and requires, among other things, a thorough understanding of the effects of magma composition on trace-element partitioning between the conjugate liquids. Further discussion of this problem is clearly beyond the scope of the present work.

4.3. Crystal fractionation?

Fractionation of olivine (Ol), low-Na calcic clinopyroxene (Cpx), nepheline (Ne), melilite (Mel) and apatite (Ap) from a hypothetical carbonate-rich silicate melt could conceivably account for the HFSE geochemistry of carbonatites, given that Nb is strongly incompatible with respect to all of the aforementioned minerals, and

that clinopyroxene is capable of decoupling Ta from Nb and Hf from Zr in the course of fractionation (Lundstrom et al., 1998; our Table 3). Products of fractionation would also have to include a capacious repository for Ti to explain a nearly ten-fold drop in Ti abundance from the silicate suite to carbonatites (Table 2). Both titaniferous magnetite (Mgt) and perovskite (Prv) are characteristic accessory and, locally, rock-forming constituents of ultramafic, melilitic and silica-undersaturated alkaline rocks at Kola and elsewhere (e.g., Kukharenko et al., 1965; Kapustin, 1986; Chakhmouradian and Mitchell, 1997) and, thus, can act as such a repository. To assess the possibility that carbonatitic magmas originate from carbonate-rich silicate melts of mantle provenance, we modeled variations in HFSE budget of the residual melt depending on the makeup of fractionating assemblage (Table 3, Fig. 3a, b). The $^{Cpx/L}D_{HFSE}$ values used in this assessment are taken from the experimental data of Skulski et al. (1994) for the Hirschfield nephelinite, whose major-element composition is similar to the hypothetical parental magma composition proposed by Kukharenko et al. (1965) and Arzamastsev et al. (2001). These values are remarkably close to the average of various experimental and empirical data for alkali-rich silica-undersaturated systems (Onuma et al., 1981; Hauri et al., 1994; Blundy et al., 1998; Lundstrom et al., 1998; Schmidt et al., 1999; Blundy and Dalton, 2000; Thompson and Malpas, 2000; Downes et al., 2004; Foley and Jenner, 2004; Plá Cid et al., 2005). The published $^{Ol/L}D_{Ti}$ values are in mutual agreement, whereas the available partition coefficients for Nb, Zr and Hf vary within one order of magnitude. Given the overall low HFSE contents of olivine and the presence in our models of phases with much higher compatibility for HFSE, these variations have no significant effect on the calculated HFSE budget. In this work, we used the data of Zanetti et al. (2004) for a hydrous basanite melt; using lower-D values (e.g., Kennedy et al., 1993) will increase the Nb, Zr and Hf contents listed in Table 3 by $\leq 0.1\%$. The HFSE partition coefficients for magnetite were taken from the data of Nielsen and Beard (2000) for alkali basalts containing magnetite with Ti, Al and Mg contents similar to those found in titaniferous magnetite from the Kola alkali-ultramafic rocks (e.g., Chakhmouradian and Zaitsev, 2004). The partitioning behavior of HFSE with respect to Prv, baddeleyite (Bad) and titanite (Ttn) has been well constrained by the recent experimental work of Corgne and Wood (2005), Klemme and Meyer (2003) and Prowatke and Klemme (2005), respectively. Their data were used in all cases, except for $^{Prv/L}D_{Ti}$, where the empirically derived

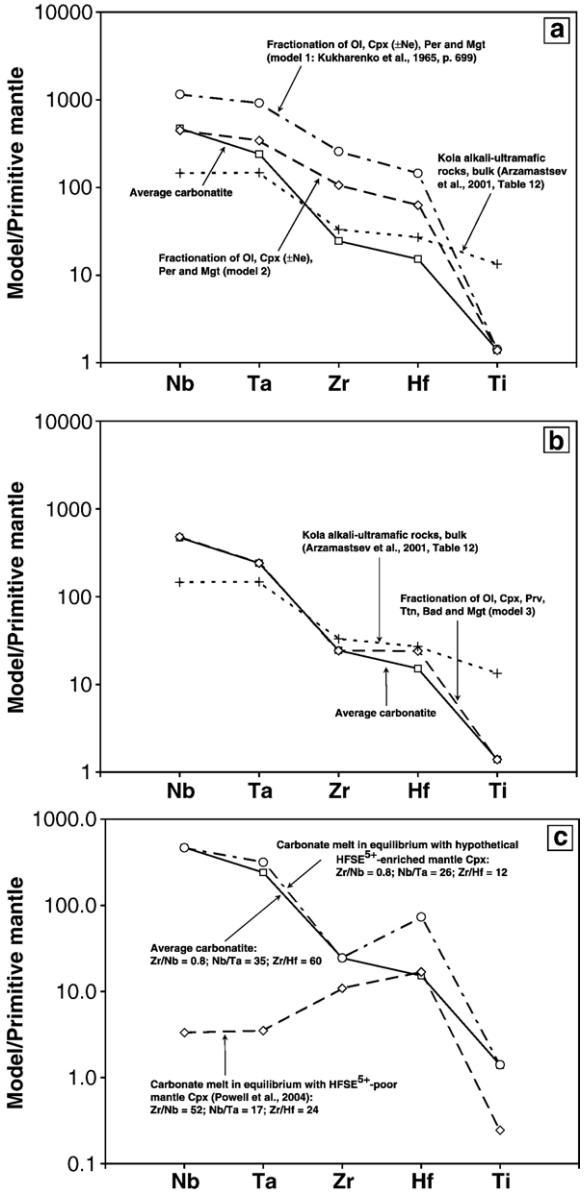

Fig. 3. HFSE budget of the average carbonatite (squares) in comparison with the composition of Kola alkali-ultramafic rocks (crosses) and model carbonate melts. (a) Melts derived from a hypothetical carbonate-rich nephelinitic parent by fractionation of various proportions of olivine (Ol), clinopyroxene (Cpx), nepheline (Ne), perovskite (Prv) and titaniferous magnetite (Mgt); (b) as in (a), but with addition of minor baddeleyite (Bad) and titanite (Ttn) to the fractionating assemblage; (c) low-degree (0.5%) partial melts in equilibrium with a carbonated lherzolite containing "normal" lherzolitic Cpx (average type-B composition of Powell et al., 2004) and best-fit model requiring an anomalously Nb–Ta-rich Cpx in the source. In (a) and (b), initial HFSE abundances as in the bulk for Kola alkali-ultramafic rocks (Arzamastsev et al., 2001); fractional melting was assumed for (c), but batch-melting calculations give nearly identical results at small F. For further details and discussion, refer to Sections 4.2 4.3 and 4.4, Tables 3 and 4.

value of Onuma et al. (1981) for the Nyiragongo nephelinite was used instead. For titanite, only the results for low-alkali, high-Al melts (ASI250, 260, 280) were averaged to calculate the $^{Ttn/L}D_{HFSE}$ values listed in Table 3. Partitioning of HFSE between nepheline, melilite and melt is poorly constrained. The very limited data available in the literature indicate that $^{Ne/L}D_{HFSE}$ are similar to, but slightly higher than, those for olivine (Onuma et al., 1981). This observation seems counter-intuitive because the structure of nepheline lacks octahedrally-coordinated sites capable of accommodating medium-sized cations; substitution of HFSE for Al or Si in the tetrahedra is highly unlikely. Hence, nepheline was not included in any of our models; the small proportion of HFSE bound in this mineral can be accounted for by excess olivine (see below). Melilite apparently has a lower capacity for HFSE than clinopyroxene (Onuma et al., 1981; Kuehner et al., 1989), although the published data are too scarce to be confidently used in petrogenetic modeling. The proportion of melilite relative to the total volume of the alkali-ultramafic suite is small ($\ll$5 vol.%: Kukharenko et al., 1965, their Table 197), and introducing this mineral into any of the models in Table 3 will only marginally affect the percent breakdown between olivine and clinopyroxene.

The average normative composition of the hypothetical parental melt, calculated by Kukharenko et al. (1965, p. 699) for Kola, is (wt.%): 41% Cpx, 29% Ol, 17% Ne, 7% Mgt, 5% Prv and 1% Ap. Model 1, based on this estimate and combining Ol with Ne and Ap, gives a reasonable Ti value, but unrealistically high contents of other HFSE at 10% of the residual melt (which roughly corresponds to the proportion of carbonatites relative to their associated alkali-ultramafic rocks). In addition, the Nb/Ta and Zr/Nb ratios in the residual melt are similar to those in the silicate rocks and markedly different from the Nb-enriched values characteristic of the carbonatites (Table 3, Fig. 3a). Model 2, which has a slightly modified proportion of the four major phases in the fractionation assemblage (Cpx, Ol, Mgt and Prv), gives a reasonable estimate for Ti, Nb and Ta contents, if a somewhat lower Nb/Ta value than in the average carbonatite. The two serious problems with this model are the unrealistically high levels of Zr and Hf in the residual carbonatite melt and the large proportion of the latter relative to the silicate-oxide assemblage (1 to 3). Even if we assume that only a relatively small percentage (ca. 25%) of the alkali-ultramafic rocks are genetically related to the associated carbonatites, as inherently implied by this model, the high Zr+Hf values (4 times the actual abundances of these elements in the carbonatites) remain inexplicable.

Other potentially significant HFSE hosts, not included in the above models, but commonly present in alkali-ultramafic rocks, are phlogopite (Phl) and calcic amphiboles (Amp). Phlogopite is much more abundant than amphiboles (particularly, in certain melilitolites and foidolites), but, by and large, still not as abundant as magnetite. Although accurate estimates of Phl+Amp contribution to the modal composition of the silicate rocks associated with carbonatites at Kola or elsewhere are not available, the actual numbers would be of little relevance to the case at hand because Zr is mildly (Amp) to strongly (Phl) incompatible with respect to both these minerals in a wide spectrum of alkaline silica-undersaturated melts (LaTourrette et al., 1995; Hilyard et al., 2000; Adam and Green, 2003; Plá Cid et al., 2005). The experimentally determined $^{Phl/L}D_{Nb}$ values are appreciably higher than $^{Phl/L}D_{Zr}$, whereas $^{Amp/L}D_{Nb} \approx {}^{Amp/L}D_{Zr}$ (ibid.), which implies that fractionation of phlogopite (with or without amphibole) from a hypothetical carbonate–silicate melt with a mantle-like HFSE signature will produce derivative magmas with high Zr/Nb ratios ($\geq$4), i.e. quite distinct from the average carbonatite.

Because Zr and Hf are incompatible with respect to all major rock-forming silicates, perovskite and magnetite, fractionation of these minerals alone cannot explain the relative depletion of carbonatites in these elements, and hence, the fractionating assemblage must include a phase (or phases) with Zr and Hf partition coefficients well in excess of 1. The most obvious choice is titanite and/or baddeleyite, both of which are compatible with respect to all HFSE (Klemme and Meyer, 2003; Prowatke and Klemme, 2005) and are known to occur in the Kola alkali-ultramafic rocks and carbonatites (Kukharenko et al., 1965; Chakhmouradian and Williams, 2004). According to the available experimental evidence, zircon does not effectively fractionate Hf from Zr in weakly polymerized melts (Linnen and Keppler, 2002), which is consistent with our data (Table 1). The best fit between the predicted and average HFSE abundances is represented by model 3 (Table 3, Fig. 3b). The two most obvious shortcomings of this model are the high proportion of fractionated titanite and baddeleyite required to bring the Zr and Hf abundances in the evolved melt to a reasonable level, and the low Zr/Hf ratio in the melt inconsistent with the Hf-depleted signature of *all* carbonatitic rocks (Table 2). The estimated weight fractions of baddeleyite and titanite relative to the silicates, perovskite and magnetite far exceed their actual contents in alkali-ultramafic rocks. Even if titanite and baddeleyite were removed after the bulk of the silicate rocks to form HFSE-rich phoscorites and silicocarbonatites, the content of these minerals would have to be

on the order of several wt.%, which is one order of magnitude higher than the maximum titanite and baddeleyite contents recorded in these rocks to date (Kukharenko et al., 1965, p. 145; Krasnova et al., 2004). It is also noteworthy that many carbonatite occurrences at Kola and elsewhere are not accompanied by any phoscorites or silicocarbonatites.

Carbonatites accompanied by consanguineous phoscorites or silicocarbonatites have a HFSE signature modified by fractionation of HFSE minerals early in the evolution of their parental magmas. Because both Ta and Hf are considerably more refractory than their homologues (Appendix A), early liquidus phases will typically be relatively enriched in heavy HFSE (Table 1). Hence, crystal fractionation will, in most cases, not only deplete the melt of HFSE, but will also modify its Nb/Ta and Zr/Hf ratios (e.g., Fig. 4). Primary perovskite, U-rich pyrochlore, baddeleyite, zirconolite and ilmenite appear to be the most effective vehicles of fractionation because they (i) are more volumetrically significant than any of the other HFSE phases, and (ii) commonly have Nb/Ta and/or Zr/Hf ratios at 50% or less of the primitive values. Crystallization of these minerals will generate a HFSE- and, especially, Ta–Hf-depleted signature in progressively more evolved types of carbonatites. This conclusion is in accord with the general trend of decreasing HFSE abundances from silicocarbonatites and phoscorites to calciocarbonatites to magnesiocarbonatites (see Section 2.2). However, the dataset used in the present work does not discriminate between magnesiocarbonatites and ferrocarbonatites that evolved from a more calcic parent, and those that represent primary magmas. Such a distinction is simply not possible at present because this aspect of carbonatite petrogenesis is not adequately addressed in the surveyed literature. It is, thus, to be expected that some of the magnesiocarbonatites and ferrocarbonatites included in the present survey are geochemically unevolved and "skew" the calculated HFSE abundances to higher values. Further studies of the trace-element geochemistry of genetically related carbonatitic rocks are required to establish with certainty whether they do indeed show a trend of decreasing HFSE abundances and increasing Nb/Ta and Zr/Hf ratios from the most primitive members of the series to the more evolved.

Fractionation of HFSE phases from carbonatitic magma cannot adequately explain why carbonatites en masse are: (i) enriched in $HFSE^{5+}$ relative to $HFSE^{4+}$ (given that Nb-rich minerals, such as perovskites, pyrochlores and ilmenite, are far more common in early cumulate facies than baddeleyite), and (ii) depleted in Ta and Hf relative to Nb and Ta. Also, the average Zr/Hf ratio of phoscorites and silicocarbonatites (57) significantly exceeds the primitive-mantle value, implying that the bulk of these rocks derive from relatively evolved magmas.

4.4. HFSE fractionation in the mantle?

An alternative view on the origin of carbonatites holds that they are derived from an independent source or sources in the upper mantle by near-solidus melting of a carbonated lherzolite at pressures above about 20 kbar (for amphibole- and phlogopite-bearing compositions: Wallace and Green, 1988; Sweeney, 1994). This model will now be tested from the standpoint of HFSE geochemistry. Phase relationships relevant to the following discussion are reproduced in Fig. 5, which was adapted largely from the experimental work of Wallace and Green (1988).

The trace-element geochemistry of mantle-derived magmas may be affected by element fractionation in the course of partial melting or by reactions with wallrock peridotite during their ascent. Blundy and Dalton (2000) have proposed that dolomitic melts generated by low-degree partial melting of carbonated lherzolite will be enriched in LREE relative to heavy REE and depleted in Ti and Zr relative to Nb owing to the appreciable differences in clinopyroxene-melt partition coefficients for

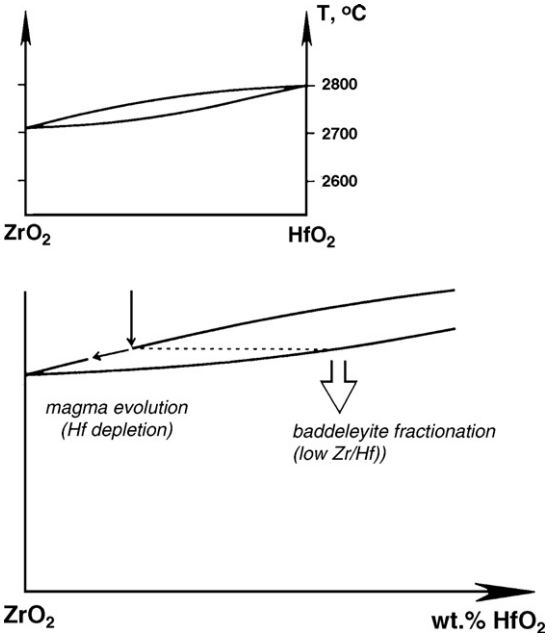

Fig. 4. Simplified phase diagram for $(Zr,Hf)O_2$ (after Yamada et al., 1988) explaining how fractionation of baddeleyite affects the HFSE budget of carbonatitic magma. Note that the liquidus and solidus temperatures will be significantly lower in natural systems. Similar relationships are observed in solid solutions involving Nb and Ta end-members (see Appendix A for examples).

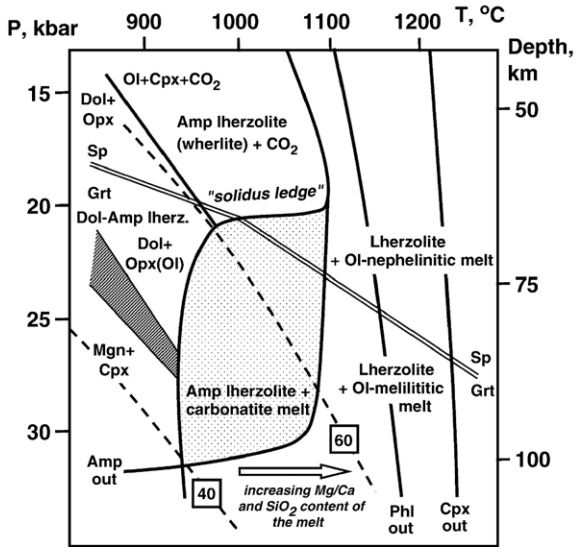

Fig. 5. Phase relationships in metasomatized lherzolitic mantle (Wallace and Green, 1988; with minor modifications and additions from Yaxley and Green, 1996; Moore and Wood, 1998). Stippled area shows where carbonatitic magmas are in equilibrium with amphibole lherzolite. Cross-hatched field and solid line to the left of the stippled field delineate equilibria among mantle carbonates, CO_2 and silicates. Double solid line separates the stability fields of spinel and garnet. Dashed lines correspond to the typical "shield" geotherm at 40 mW/m^2 (lower) and hotter, "oceanic" geotherm at 60 mW/m^2 (Menzies and Chazot, 1995). Symbols: Amp=amphibole, Cpx=calcic clinopyroxene, Dol=dolomite, Grt=garnet, Mgn=magnesite, Ol=olivine, Opx=orthopyroxene, Sp=spinel.

these elements (Table 4). To test this possibility, we calculated the HFSE budget of a carbonate melt in equilibrium with lherzolite using the experimental data of Klemme et al. (1995). Their partition coefficients are in general agreement with those determined by Blundy and Dalton (2000) and Green et al. (1992), but include data for both Zr and Hf obtained from the same sample. In order for the HFSE budget of a model carbonate melt to approach that of the average carbonatite, the clinopyroxene in equilibrium with the melt should contain on the order of 2000 ppm Ti, 100 ppm Zr, 30 ppm Nb and several ppm Ta and Hf. Even a cursory survey of the literature shows that, although mantle clinopyroxenes do commonly exhibit the required level of $HFSE^{4+}$ enrichment, their Nb and Ta contents are one to two orders of magnitude lower than required (e.g., Powell et al., 2004; Akinin et al., 2005; Plá Cid et al., 2005). Using the lower partition coefficients for $HFSE^{5+}$ (Green et al., 1992; Coltorti et al., 1999) still yields Nb and Ta abundances one order of magnitude lower than what should be expected for primitive carbonatitic magmas. Thus, although $HFSE^{5+}$ are more compatible with respect to carbonate melts than $HFSE^{4+}$, the paucity of Nb and Ta in mantle clinopyroxene will result in overall low concentrations of these elements and, consequently, high Zr/Nb ratios in such melts (Fig. 3c).

Another critical observation concerns the contrasting partitioning behavior of Ta and Hf with respect to their "twin pairs": $^{Cpx/Carb}D_{Ta}$ is higher than $^{Cpx/Carb}D_{Nb}$, whereas $^{Cpx/Carb}D_{Hf}$ and $^{Cpx/Carb}D_{Zr}$ show the reverse relationship (Green et al., 1992; Klemme et al., 1995). At low degrees of melting (<5%), a melt derived from carbonated lherzolite will likely have an Nb/Ta ratio appreciably higher and a Zr/Hf ratio lower than the primitive-mantle values, and a mirroring distribution of these elements in the residual clinopyroxene. This prediction is readily confirmed by the HFSE patterns of peridotitic clinopyroxene equilibrated with carbonate-rich melts (e.g., Nb/Ta=11 and Zr/Hf=70 in type-B xenoliths of Powell et al., 2004; Nb/Ta=12 and Zr/Hf=74 in Kerguelen material of Delpech et al., 2004), but is at variance with the actual geochemistry of carbonatitic rocks, which consistently show a Hf-depleted signature (Table 2, Fig. 3c). Hence, we propose that the bulk of carbonatites must be derived from an $HFSE^{5+}$-enriched (metasomatized) mantle source with Nb/Ta and Zr/Hf ratios *significantly enhanced* relative to the primitive-mantle values.

By modeling the partitioning of trace elements, Arzamastsev et al. (2001) have shown that the Devonian alkaline magmas at Kola originated by very low-degree (<1%) partial melting of enriched garnet lherzolite. Evidence for metasomatic enrichment preceding the melting is many-fold, and includes trace-element and isotopic compositions of primitive alkali-ultramafic rocks across the region, and the mineralogy of upper-mantle and lower-crust xenoliths (e.g., Beard et al., 1998; Kempton et al., 2001; Vetrin et al., 2003). The metasomatism is believed to have been involved in the crystallization of hydrous alkali silicates, phlogopite and amphibole, serving as the principal hosts for HFSE (Arzamastsev et al., 2001). However, due to the limited amount of xenolithic material available for study, the actual composition of the mantle source(s) can only be speculated upon.

The crystal chemistry of mantle amphiboles (such as titanian pargasite or kaersutite) makes them a better sink for $HFSE^{5+}$ than clinopyroxene (Gregoire et al., 2000b; Powell et al., 2004), and an effective vehicle of Nb+Ta vs. Zr+Hf fractionation (Tiepolo et al., 2001). Interestingly, the most primitive, high-Ti amphiboles from upper-mantle xenoliths worldwide exhibit compositional characteristics broadly similar to the magmas parental with respect to the Kola alkali-ultramafic rocks (i.e., mantle-like Nb/Ta and Zr/Hf, but Zr/Nb ≤ 4 and Zr/Ta ≤ 70) (Table 4 and references therein). The importance of

Table 4
HFSE in the Earth's mantle: ratios and relevant partition coefficients

	Element ratios				Data sources
	Nb/Ta	Zr/Hf	Zr/Nb	Zr/Ta	
Primitive mantle	18	37	16	284	McDonough and Sun (1995)
Alkali-ultramafic complexes (Kola)	17	46	3.6	63	Arzamastsev et al. (2001)
Carbonatites [a]	35	60	0.8	29	This work
Mantle amphiboles:					
Argentina					
early high-Ti	19	38	3.6	70	Laurora et al. (2001)
late low-Ti	38	205	0.3	11	
Australia					
high-Ti	18	36	3.0	55	Yaxley and Kamenetsky (1999)
low-Ti	30	60	1.1	34	
Kerguelen					
high-Ti	19	40	2.3	45	Moine et al. (2001)
interstitial	21	53	2.1	45	
Siberia					
high-Ti	19	29	2.0	38	Ionov and Hofmann (1995)
Spitsbergen					
high-Ti	16	25	1.2	19	Ionov et al. (2002)

Partition coefficients [b]	Ti	Nb	Ta	Zr	Hf	Data sources
$^{Cpx/Carb}D$ (exp, 20–22 kbar, 1050–1100 °C)	1.42	0.10 [c]	0.15[c]	0.48	0.16	Klemme et al. (1995)
$^{Amp/Carb}D$ (exp, 18 kbar, 960 °C, 2% H_2O)	6.1	0.31	0.86	1.18	–	Sweeney et al. (1992)
$^{Phl/Carb}D$ (exp, 18 kbar, 1200 °C)	2.1	0.09	0.21	0.05	–	Sweeney et al. (1995)
$^{Phl/Carb}D$ (emp)	2.87	3.91	2.40	0.015	0.005	Gregoire et al. (2000a,b)
$^{Amp/Cpx}D$ (emp)	4.86	24.64	5.17	0.91	0.45	ibid.
$^{Phl/Cpx}D$ (emp)	7.61	76.00	24.56	0.30	0.19	ibid.
$^{Phl/Amp}D$ (emp)	1.52	2.09	3.14	0.30	0.17	ibid.
$^{Phl/Amp}D$ (emp)	1.19	0.48	0.50	0.05	0.06	Moine et al. (2001)
$^{Ilm/Amp}D$ (emp)	6.0	7.2	16.1	1.2	0.7	ibid.

[a] See footnote to Table 3.
[b] Partition coefficients (D) for calcic clinopyroxene (Cpx), pargasitic amphibole (Amp), phlogopite (Phl) and ilmenite (Ilm) relative to one another and to carbonate melt below the solidus ledge.
[c] Green et al. (1992) report significantly lower values which still show $^{Cpx/Carb}D_{Ta} > {}^{Cpx/Carb}D_{Nb}$.

amphiboles as a repository and source of HFSE in the processes of metasomatism and melting in the mantle has been previously recognized in numerous studies (Wallace and Green, 1988; Sweeney et al., 1992; Laurora et al., 2001; Späth et al., 2001, among others). With increasing degrees of partial melting, more refractory HFSE repositories (especially, phlogopite, clinopyroxene and titanates) may become significant, changing the trace-element budget of a melt. Xenoliths of pargasite-bearing peridotites and xenocrystic pargasite have been found in extrusive alkali-ultramafic rocks and carbonatites at several Kola localities (Arzamastsev and Dahlgren, 1994; Vetrin et al., 2003). There is also geochemical evidence that some of the alkali-ultramafic silicate rocks in the Province crystallized from magmas generated by near-solidus partial melting of amphibole-bearing peridotite (Chakhmouradian and Zaitsev, 2004). The nature and source of metasomatizing melts (fluids?) is debatable, although models involving interaction of the subcontinental lithosphere with a lower-mantle plume have thus far prevailed (Beard et al., 1998; Arzamastsev et al., 2001; Tolstikhin et al., 2002; Sindern et al., 2004). Additional contributions from sources other than a plume have been proposed on the basis of isotopic data by Dunworth and Bell (2001).

In the stability range of carbonate melts, HFSE exhibit a fairly complex partitioning behavior with respect to both pargasitic amphibole and phlogopite (Table 4). In general, the mineral-melt partition coefficients increase with decreasing pressure and H_2O content (e.g., Sweeney et al., 1992). Hence, a carbonate (Na-rich dolomitic) melt rising through the lithosphere will fractionate Nb, Ta, Zr and Hf by equilibrating with mantle peridotites and producing hydrous alkali silicates and, possibly, other phases enriched in these elements. Differences in partition coefficients for individual HFSE will affect the chemical

evolution of both ascending melts and metasomatized mantle rocks (e.g., Ionov et al., 2002). Any petrogenetic model implying carbonatite lineage from a discrete (in a petrologic, not isotopic, sense) mantle source must explain very low Zr/Nb and Zr/Ta ratios, as well as high Nb/Ta and Zr/Hf ratios in the carbonatites in comparison with the associated alkaline-ultramafic rocks (Table 4).

According to the published xenolith studies, mantle amphiboles are capable of fractionating HFSE not only between, but also within the "geochemical twin" pairs, in some cases changing the Nb/Ta or Zr/Hf ratio by a factor of 3 across a distance of several cm (e.g., Moine et al., 2001, their Table 6). In those cases where the formation of amphiboles is attributed to carbonate metasomatism, these minerals become progressively enriched in Nb and depleted in Ti, Zr and Hf, lowering the Zr/HFSE^{5+} and increasing the Nb/Ta and Zr/Hf ratios (Laurora et al., 2001). A progressive increase in Nb/Zr ratio has been also observed in pargasite/kaersutite equilibrated with alkali-basaltic melts in experimental systems (Tiepolo et al., 2001), indicating that this partitioning behavior is controlled by the crystal chemistry of amphibole rather than the properties of a melt. Note that a very similar trend marks transition from the Kola alkali-ultramafic magmas to carbonatites (Table 4). The amphibole-induced trace-element signature may be counterbalanced by co-crystallization of phlogopite and Ti oxides in the wallrock, which show different (but, at present, poorly constrained) partitioning behaviors (Table 4). The lack of potassic alkaline rocks in the carbonatite milieu and the distinct K–Rb-depleted signature of Kola carbonatites (Ivanikov et al., 1998; Chakhmouradian and Zaitsev, 2004; Lee et al., 2004; Zaitsev et al., 2004) imply that phlogopite remained refractory during the extraction of carbonatitic magmas. Although the presence of HFSE oxides (such as rutile, Mg-rich ilmenite, or armalcolite) in the mantle source cannot be ruled out, these minerals are stable well above the amphibole and phlogopite solidi (e.g., Gregoire et al., 2000a). Rutile, interpreted to be the principal Nb–Ta host in some spinel peridotites (e.g., ibid.; Bodinier et al., 1996; Kalfoun et al., 2002), will remain refractory anywhere in the stippled area in Fig. 5, which would undoubtedly manifest itself in the HFSE budget of carbonatitic magmas tapping a rutile-bearing source (see below).

5. Integrated petrogenetic model

One major implication of the preceding discussion is that the HFSE geochemistry of carbonatites en masse offers no convincing evidence to support their common lineage with associated alkali-ultramafic rocks. On a cautionary note, however, some carbonatites *do* exhibit depletion in all, or certain groups of, HFSE and concomitant enrichment in Sr, Ba and LREE relative to the associated silicate suite, which is consistent with their derivation from a common parent by either immiscibility or crystal fractionation. Such special cases, however, cannot be extrapolated to a broader geological context.

Another important implication is that the HFSE signature of carbonatites and associated silicate rocks can be generated by a *single* process, i.e. HFSE^{4+} and heavy-HFSE fractionation induced by metasomatic processes in the mantle (Fig. 6). The available mineralogical, geochemical and experimental evidence indicates that metasomatic crystallization of amphibole is a probable and certainly a very effective vehicle of such fractionation. The early generations of amphibole will preferentially concentrate HFSE^{4+} (relative to HFSE^{5+}), causing enrichment of the percolating melt in Nb and Ta (Laurora et al., 2001; Tiepolo et al., 2001). More evolved amphiboles will contain a higher proportion of HFSE^{5+} as these elements become more compatible with respect to the amphibole structure under decreasing pressure and H_2O content (Sweeney et al., 1992), and the availability of HFSE^{4+} in the melt decreases. The Nb/Ta and Zr/Hf ratios will initially be near or below the primitive-mantle values (owing to the more refractory character of the heavy HFSE and their higher compatibility for amphibole), but should increase progressively with metasomatism. The absolute values of the amphibole-melt partition coefficients for individual elements should be used with caution, because they will vary significantly depending on the composition and structure of the melt, concentration and speciation of an element, and crystallographic and paragenetic constraints (for discussion, see Laurora et al., 2001; Moine et al., 2001). However, the general trends outlined above for the HFSE ratios are not likely to change much, as indicated by the similarity of amphiboles generated by different types of metasomatism in various mantle rocks (Table 4).

As noted above, the nature of metasomatizing agent(s) is uncertain, but it is conceivable that the hypothetical amphibole-enriched sources were produced by reaction of garnet lherzolite with plume-derived carbonate melts. The major arguments in favor of this surmise are that:

(i) Involvement of carbonate melts is the most obvious means to account for relatively voluminous carbonatite magmatism at Kola (see above);

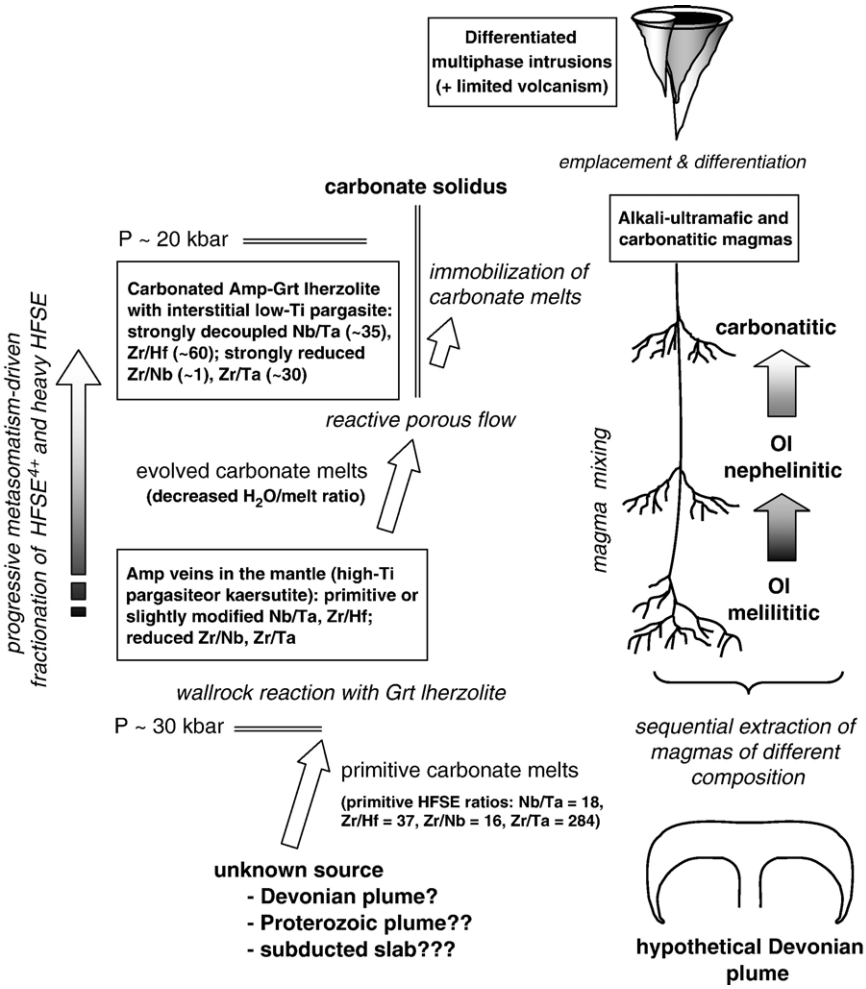

Fig. 6. Proposed petrogenetic model for the carbonatite–alkali–ultramafic rock association at Kola. Pressure-temperature constraints are based on the experimental data of Wallace and Green (1988); refer to Fig. 5 for relevant phase equilibria and symbols. For a detailed discussion, see Sections 4.4 and 5.

(ii) The weighted average composition of the Kola alkali-ultramafic complexes (Arzamastsev et al., 2001, their Fig. 7b) shows depletion of $HFSE^{4+}$ (but not Nb) relative to LREE and Sr; this trace-element signature is considered a "hallmark" of carbonate metasomatism (Sweeney et al., 1995; Coltorti et al., 1999; Neumann et al., 2002);

(iii) Equilibration of a carbonate (Na-rich dolomitic) melt with lherzolite is known to produce amphiboles in the pargasite–kaersutite–edenite compositional range (e.g., Yaxley and Green, 1996; Yaxley et al., 1998);

(iv) In the 21–30 kbar pressure range, the carbonate solidus lies significantly below that of the least refractory silicate phase — amphibole (Wallace and Green, 1988), i.e. carbonate melts are more readily produced than any of the alkali–silicate melts that could potentially serve as alternative agents of metasomatism (cf. Moine et al., 2001).

Note that these hypothetical carbonate melts are not equivalent to those that were eventually emplaced in the crust to produce carbonatitic rocks (to emphasize the distinction, the latter are referred to here as carbonatitic magmas). Had the primitive melts reached crustal levels, carbonatitic rocks would have predated all other types of magmatism originating in metasomatized mantle sources. In contrast, the Kola carbonatites show cross-cutting relationships with respect to all or most of the ultramafic and alkaline intrusive series found at the same locality (e.g., Lapin, 1979; Ivanikov et al., 1998). Carbonatite–silicate rock associations elsewhere in the

world typically show similar temporal relationships (e.g., Kapustin, 1986; Egorov, 1991).

Evidently, the extent of metasomatism would be limited by the carbonate solidus at ca. 950 °C and decarbonation of the melt at the "solidus ledge", i.e. below about 20 kbar (Wallace and Green, 1988; Yaxley and Green, 1996; Fig. 4). Some of the melts should cross into the dolomite stability field as they cool and lose H_2O, and give rise to carbonated garnet lherzolite. Thus, metasomatism of the Kola lithospheric mantle over a range of pressures by ascending carbonate melts could produce an enriched lherzolitic reservoir with heterogeneous HFSE distribution, capable of producing a wide spectrum of alkali-ultramafic and carbonatitic magmas. Within this source, varying degrees of partial melting at different depths produced magmas ranging from olivine-melilititic to (mela)nephelinitic to carbonatitic in composition. The carbonatitic magmas were derived from carbonated mantle assemblages (e.g., dolomite-amphibole-bearing garnet lherzolite) nearly contemporaneously with, or following the extraction of alkali-ultramafic melts from deeper levels of the metasomatized mantle. Note that the CO_2-poor silicate magmas were sufficiently hot in order to bypass the "solidus ledge", whereas most carbonatitic magmas probably had to re-equilibrate with spinel lherzolite at these depths. More detailed discussions of the significance of these processes for carbonatite petrogenesis can be found in Yaxley and Green (1996), Moore and Wood (1998), Wyllie and Lee (1998), and Lee and Wyllie (2000).

There seems little doubt that some carbonatitic magmas undergo fractionation at crustal levels, producing silicate-rich cumulate rocks with a high modal content of HFSE phases (e.g., phoscorites) and carbonatites further depleted in Ta and Hf (e.g., Veksler et al., 1998a,b; Chakhmouradian and Zaitsev, 2004; Lee et al., 2004). The significance and extent of liquid immiscibility in the evolution of carbonatitic magmas remain to be determined. Carbonate-rich silicate magmas may evolve either to the silicate–carbonate liquidus boundary (path 2 of Lee and Wyllie, 1998b) or to alkali-rich compositions at the immiscibility gap (path 3), eventually yielding minor volumes of carbonatitic rocks. These derivative types of carbonatites can be discriminated not only using petrographic and mineralogical criteria, but also on the basis of their trace-element geochemistry, particularly in relation to the associated silicate lithologies (see Sections 4.1 and 4.2 above). As there is no evidence for geochemical bimodality (Fig. 1), the proportion of such derivative carbonatites is probably quite small on the global scale.

The proposed petrogenetic model is summarized in Fig. 6. It is consistent with the highly fractionated HFSE signature of carbonatitic rocks relative to the primitive mantle and coeval alkali-ultramafic series, the generally older age of the latter, the previous estimates of magma-generation depths (Ivanikov et al., 1998; Arzamastsev et al., 2001), and the fact that both carbonate and silicate rocks show contributions from a primitive sublithospheric source (e.g., the hypothetical mantle plume: Dunworth and Bell, 2001; Tolstikhin et al., 2002). The estimated plume input to the upper-mantle reservoir is on the order of 2 wt.% (Tolstikhin et al., 2002), i.e. remarkably close to the proportion of carbonatites among the products of Paleozoic magmatism (Arzamastsev et al., 2001). This numerical similarity may not be coincidental, and may instead indicate that nearly all of the carbonate material involved in the metasomatism was subsequently extracted from the lithospheric reservoir as carbonatitic magmas. Such efficiency can be expected where mantle metasomatism and melting are contiguous in space and time; e.g., if both processes were connected to the same Devonian plume (for relevant time and size constraints, see Arzamastsev et al., 2001). This conjecture is in accord with Kramm et al.'s (1993) finding that the mantle enrichment occurred shortly prior to the extraction of alkaline melts. The rising plume and related tectonic processes (such as lithospheric erosion and crust thinning) eventually raised the cool "shield" geotherm enough to initiate melting (Fig. 5).

A few important remarks should be made with regard to Fig. 6. Although the provenance of metasomatizing melts (fluids?) is speculative (e.g., Chakhmouradian and Zaitsev, 2004), the HFSE geochemistry of the Kola Devonian complexes makes subducted material a very unlikely source. It is well established experimentally that refractory rutile in the subducted slab will retain HFSE and especially Nb + Ta, thereby producing a distinct $HFSE^{5+}$-depleted signature in the slab-derived melts (Dalton and Blundy, 2000; Foley et al., 2000; Green, 2000). Carbonatites from craton-margin settings affected by slab recycling should show noticeable depletion in Nb relative to Zr. The low Zr/Nb ratio of the Kola carbonatites, which is nearly identical to that of the average carbonatite and much lower than the primitive-mantle value (Table 3), indicates that such depletion did not occur. For the reasons discussed in the previous paragraph, any of the Precambrian plumes that might have affected the Kola lithosphere (Kempton et al., 2001) could probably also be ruled out as the principal source of metasomatizing melts.

Another comment refers to the right-hand side of Fig. 6. For simplicity, only the major magma types are shown in this part of the diagram, whereas magma mixing and tapping of the lithospheric reservoir at intermediate

depths likely resulted in a much broader spectrum of melts, including transitional types (e.g., melilite–nephelinitic, alnöitic, etc.). Such a suggestion would be in accord with the experimental findings that a continuous series of magmas with differing CO_2, SiO_2, Mg and Ca contents can be produced by different degrees of melting above the "solidus ledge" (e.g., Moore and Wood, 1998). In summary, polybaric tapping of a heterogeneous mantle reservoir, combined with subsequent mixing and differentiation of the magmas so produced, can potentially account for the diversity of alkaline-ultramafic rocks observed at Kola, as well as for the age relationships of individual petrographic series.

6. Conclusion

We would like to point out that the model proposed here is probably valid for intracratonic carbonatite-alkali-ultramafic rock associations beyond Kola, but it certainly has limited applicability to other types of tectonic settings (e.g., carbonatites in cratonic margins underplated by subducted crust), or other types of rock associations (e.g., Sr–Ba-rich "carbonatites", see Section 2.2). To date, these relatively rare types of carbonatites have not been studied in adequate detail. A far more vigorous study of carbonatitic rocks from different tectonic–igneous environments, and preferably involving a broader range of characteristic trace elements (especially Th, U, REE, Sr and Ba), would be essential for achieving a better understanding of the early evolution of carbonatitic magmas.

Acknowledgements

This study was inspired by the tireless work of the "carbonatite-minded" experimental petrologists around the globe, and that of many Russian geologists at Kola and other alkaline provinces. Ilya Veksler, Hilary Downes, an anonymous referee and Editor Steven L. Goldstein are thanked for their insightful and constructive reviews of the earlier drafts of this paper, and Mario Bieringer for his valuable comments on the chemistry of HFSE. The National Sciences and Engineering Research Council of Canada, and the University of Manitoba are gratefully acknowledged for their support.

Appendix A. Supplementary data

Supplementary data associated with this article can be found, in the online version, at doi:10.1016/j.chemgeo.2006.06.008.

References

Adam, J., Green, T., 2003. The influence of pressure, mineral composition and water on trace element partitioning between clinopyroxene, amphibole and basanitic melts. Eur. J. Mineral. 15, 831–841.

Akinin, V.V., Sobolev, A.V., Ntaflos, Th., Richter, W., 2005. Clinopyroxene megacrysts from Enmelen melanephelinitic volcanoes (Chukchi Peninsula, Russia): application to composition and evolution of mantle melts. Contrib. Mineral. Petrol. 150, 85–101.

Andersen, T., 1988. Evolution of peralkaline calcite carbonatite magma in the Fen complex, southeast Norway. Lithos 22, 99–112.

Armbruster, T., Birrer, J., Libowitzky, E., Beran, A., 1998. Crystal chemistry of Ti-bearing andradites. Eur. J. Mineral. 10, 907–921.

Arzamastsev, A.A., Dahlgren, S., 1994. Plutonic mineral assemblages in Paleozoic dikes and explosion pipes of the alkaline province of the Baltic Shield. Geochem. Int. 31 (3), 7–68.

Arzamastsev, A.A., Bea, F., Glaznev, V.N., Arzamastseva, L.V., Montero, P., 2001. Kola alkaline province in the Paleozoic: evaluation of primary mantle magma composition and magma generation conditions. Russ. J. Earth Sci. 3 (available at http://www.agu.org/wps/rjes).

Bagdasarov, Yu.A., 1989. Composition of magnetites from carbonatite complexes and depth facies of carbonatites. In: Bagdasarov, Yu.A., Efimov, A.F. (Eds.), Forecasting and evaluating carbonatites. IMGRE, Moscow, pp. 124–156 (in Russ.).

Bagdasarov, Yu.A., 1993. Geochemical features of upper Vendian Zr-bearing dolomites, a new type of Zr ore show. Geochem. Int. 30 (7), 88–98.

Bagdasarov, Yu.A., Pukarev, S.Yu., 1989. Characteristics of inflow-outflow of rock-forming and other components during metasomatic carbonatite formation in an ultrabasic-alkaline massif, southern Siberia. In: Bagdasarov, Yu.A., Efimov, A.F. (Eds.), Forecasting and evaluating carbonatites. IMGRE, Moscow, pp. 45–55 (in Russ.).

Beard, A.D., Downes, H., Hegner, E., Sablukov, S.M., Vetrin, V.R., Balogh, K., 1998. Mineralogy and geochemistry of Devonian ultramafic minor intrusions of the southern Kola Peninsula, Russia: implications for the petrogenesis of kimberlites and melilitites. Contrib. Mineral. Petrol. 130, 288–303.

Bell, K., Simonetti, A., 1996. Carbonatite magmatism and plume activity: implications from the Nd, Pb and Sr isotope systematics of Oldoinyo Lengai. J. Petrol. 37, 1321–1339.

Blundy, J., Dalton, J., 2000. Experimental comparison of trace element partitioning between clinopyroxene and melt in carbonate and silicate systems, and implications for mantle metasomatism. Contrib. Mineral. Petrol. 139, 356–371.

Blundy, J.D., Robinson, J.A.C., Wood, B.J., 1998. Heavy REE are compatible in clinopyroxene on the spinel lherzolite solidus. Earth Planet. Sci. Lett. 160, 493–504.

Bodinier, J.-L., Merlet, C., Bedini, R.M., Simien, F., Remaidi, M., Garrido, C.J., 1996. Distribution of niobium, tantalum, and other highly incompatible trace elements in the lithospheric mantle: the spinel paradox. Geochim. Comsochim. Acta 60, 545–550.

Borisov, A.B., 1985. Mineralogy and genesis of benstonitic carbonatites of the Murun massif. Vestnik Leningr. Univer., Ser. 7. Geol. Geogr. 1985 (3), 97–102 (in Russ.).

Bulakh, A.G., Ivanikov, V.V., Orlova, M.P., 2004. Overview of carbonatite–phoscorite complexes of the Kola Alkaline Province in the context of Scandinavian North Atlantic Alkaline Province. In: Wall, F., Zaitsev, A.N. (Eds.), Phoscorites and carbonatites from mantle to mine: the key example of the Kola Alkaline Province. Mineralogical Society, London, pp. 1–43.

Bulnaev, K.B., 1996. Strontianite carbonatites of the Khalyuta deposit (western Transbaikal region, Russia). Geol. Ore Depos. 38, 390–400.

Chakhmouradian, A.R., 2004. Crystal chemistry and paragenesis of compositionally unique (Al-, Fe-, Nb- and Zr-rich) titanite from Afrikanda, Russia. Am. Mineral. 89, 1752–1762.

Chakhmouradian, A.R., McCammon, C.A., 2005. Schorlomite: a discussion of the crystal chemistry, formula, and inter-species boundaries. Phys. Chem. Mineral. 32, 277–289.

Chakhmouradian, A.R., Mitchell, R.H., 1997. Compositional variation of perovskite-group minerals from the carbonatite complexes of the Kola Alkaline Province, Russia. Can. Mineral. 35, 1293–1310.

Chakhmouradian, A.R., Williams, T.C., 2004. Mineralogy of high-field-strength elements (Ti, Nb, Zr, Ta, Hf) in phoscoritic and carbonatitic rocks of the Kola Peninsula, Russia. In: Wall, F., Zaitsev, A.N. (Eds.), Phoscorites and carbonatites from mantle to mine: the key example of the Kola Alkaline Province. Mineralogical Society, London, pp. 293–340.

Chakhmouradian, A.R., Zaitsev, A.N., 1999. Calcite-amphibole-clinopyroxene rock from the Afrikanda complex, Kola Peninsula (Russia): mineralogy and a possible link to carbonatites. I. Oxide minerals. Can. Mineral. 37, 177–198.

Chakhmouradian, A.R., Zaitsev, A.N., 2002. Calcite-amphibole-clinopyroxene rock from the Afrikanda complex, Kola Peninsula (Russia): mineralogy and a possible link to carbonatites. III. Silicate minerals. Can. Mineral. 40, 1347–1374.

Chakhmouradian, A.R., Zaitsev, A.N., 2004. Afrikanda: An association of ultramafic, alkaline and alkali-silica-rich carbonatitic rocks from mantle-derived melts. In: Wall, F., Zaitsev, A.N. (Eds.), Phoscorites and carbonatites from mantle to mine: the key example of the Kola Alkaline Province. Mineralogical Society, London, pp. 247–291.

Chakhmouradian, A.R., McCammon, C.A., MacBride, L.M., Cahill, C., 2005. Titaniferous garnets in carbonatites: their significance and place in the evolutionary history of host rocks. GAC-MAC-CSPG-CSSS Meet (Halifax, NS) Abstr., vol. 30, p. 27.

Coltorti, M., Bonadiman, C., Hinton, R.W., Siena, F., Upton, B.G.J., 1999. Carbonatite metasomatism in the oceanic upper mantle: evidence from clinopyroxenes and glasses in ultramafic xenoliths of Grande Comore, Indian Ocean. J. Petrol. 40, 133–165.

Corgne, A., Wood, B.J., 2005. Trace element partitioning and substitution mechanisms in calcium perovskites. Contrib. Mineral. Petrol. 149, 85–97.

Dalton, J., Blundy, J., 2000. Carbonatites from recycled eclogites. J. Conf. Abstr. 5, 330.

David, K., Schiano, P., Allègre, C.J., 2000. Assessment of the Zr/Hf fractionation in oceanic basalts and continental materials during petrogenetic processes. Earth Planet. Sci. Lett. 178, 285–301.

Dawson, J.B., Steele, I.M., Smith, J.V., Rivers, M.L., 1996. Minor and trace element chemistry of carbonates, apatites and magnetites in some African carbonatites. Mineral. Mag. 60, 415–425.

Delpech, G., Gregoire, M., O'Reilly, S.Y., Cottin, J.Y., Moine, B., Michon, G., Giret, A., 2004. Feldspar from carbonate-rich silicate metasomatism in the shallow oceanic mantle under Kerguelen Islands (South Indian Ocean). Lithos 75, 209–237.

Dorfman, M.D., Kapustin, Yu.L., 1991. Liquation phenomena in a carbonate dike of the Mushugai-Khuduk complex in Mongolia. Geol. Geofiz. 1991 (8), 98–102 (in Russ.).

Dostal, J., Chatterjee, A.K., 2000. Contrasting behaviour of Nb/Ta and Zr/Hf ratios in a peraluminous granitic pluton (Nova Scotia, Canada). Chem. Geol. 163, 207–218.

Downes, H., Beard, A., Hinton, R., 2004. Natural experimental charges: an ion-microprobe study of trace element distribution coefficients in glass-rich hornblendite and clinopyroxenite xenoliths. Lithos 75, 1–17.

Dunworth, E.A., Bell, K., 2001. The Turiy massif, Kola Peninsula, Russia: isotopic and geochemical evidence for multi-source evolution. J. Petrol. 42, 377–405.

Egorov, L.S., 1991. Ijolite-carbonatite plutonism. Nedra, Leningrad, Russia. 260 pp (in Russ.).

Entin, A.R., Zaitsev, A.I., Lazebnik, K.A., Nenashev, N.I., Marshintsev, V.K., Tyan, O.A., 1991. Carbonatites of Yakutia (composition, mineralogy). Yakutsk Sci. Center, Yakutsk. 240 pp (in Russ.).

Foley, S.F., Jenner, G.A., 2004. Trace element partitioning in lamproitic magmas — the Gaussberg olivine leucitite. Lithos 75, 19–38.

Foley, S.F., Barth, M.G., Jenner, G.A., 2000. Rutile/melt partition coefficients for trace elements and an assessment of the influence of rutile on the trace element characteristics of subduction zone magmas. Geochim. Cosmochim. Acta 64, 933–938.

Garanin, V.K., Kudryavsteva, G.P., Lapin, A.V., 1980. Typical features of ilmenite from kimberlites, alkali-ultrabasic intrusions, and carbonatites. Int. Geol. Rev. 22, 1025–1050.

Gaspar, J.C., Wyllie, P.J., 1983. Ilmenite (high Mg, Mn, Nb) in the carbonatites from the Jacupiranga complex. Am. Mineral. 68, 960–971.

Gendron, L., Bis, R., Rodrigue, M., 1984. Underground mining and pyrochlore ore processing at Niobec mine, Quebec, Canada. In: Stuart, H. (Ed.), Niobium, Proceed. Int. Symp. Metall. Soc. AIME, Warrendale, Pennsylvania, pp. 79–96.

Giere, R., Williams, C.T., Lumpkin, G.R., 1998. Chemical characteristics of natural zirconolite. Schweiz. Mineral. Petrogr. Mitt. 78, 433–459.

Gold, D.P., 1963. Average chemical composition of carbonatites. Econ. Geol. 58, 988–991.

Green, T.H., 2000. New partition coefficient determinations pertinent to hydrous melting processes in subduction zones. State of the Arc 2000 Conference Abstracts, New Zealand.

Green, T.H., Adam, J., Sie, S.H., 1992. Trace element partitioning between silicate minerals and carbonatite at 25 kbar and application to mantle metasomatism. Mineral. Petrol. 46, 179–184.

Gregoire, M., Lorand, J.P., O'Reilly, S.Y., Cottin, J.Y., 2000a. Armalcolite-bearing, Ti-rich metasomatic assemblages in harzburgitic xenoliths from the Kerguelen Islands: implications for the oceanic mantle budget of high-field strength elements. Geochim. Cosmochim. Acta 64, 673–694.

Gregoire, M., Moine, B.N., O'Reilly, S.Y., Cottin, J.Y., Giret, A., 2000b. Trace element residence and partitioning in mantle xenoliths metasomatized by highly alkaline, silicate- and carbonate-rich melts (Kerguelen Islands, Indian Ocean). J. Petrol. 41, 477–509.

Hauri, E.H., Wagner, T.P., Grove, T.L., 1994. Experimental and natural partitioning of Th, U, Pb and other trace elements between garnet, clinopyroxene and basaltic melts. Chem. Geol. 117, 149–166.

Hilyard, M., Nielsen, R.L., Beard, J.S., Patiño-Douce, A., Blencoe, J., 2000. Geochim. Cosmochim. Acta. 64, 1103–1120.

Ibhi, A., Nachit, H., 2000. The substitution mechanism of Ba and Ti into phyllosilicate phases: the example of barium–titanium biotite. Ann. Chim. Sci. Mater. 25, 627–634.

Ibhi, A., Nachit, H., Abia, E.H., Hernandez, J., 2002. Intervention des segregats carbonatitiques dans la petrogenèse des nephelinites à pyroxène de Jbel Saghro (Anti-Atlas, Maroc). Bull. Soc. Geol. Fr. 173, 37–43.

Ionov, D.A., Harmer, R.E., 2002. Trace element distribution in calcite–dolomite carbonatites from Spitskop: inferences for differentiation of carbonatite magmas and the origin of carbonates in mantle xenoliths. Earth Planet. Sci. Lett. 198, 495–510.

Ionov, D.A., Hofmann, A.W., 1995. Nb–Ta-rich amphiboles and micas: implications for subduction-related metasomatic trace-element fractionations. Earth Planet. Sci. Lett. 131, 341–356.

Ionov, D.A., Bodinier, J.-L., Mukasa, S., Zanetti, A., 2002. Mechanisms and sources of mantle metasomatism: major and trace element compositions of peridotite xenoliths from Spitsbergen in the context of numerical modelling. J. Petrol. 43, 2219–2259.

Ivanikov, V.V., Rukhlov, A.S., Bell, K., 1998. Magmatic evolution of the melilitite–carbonatite–nephelinite dike series of the Turiy Peninsula (Kandalaksha Bay, White Sea, Russia). J. Petrol. 39, 2043–2059.

Ivanyuk, G.Yu., Yakovenchuk, V.N., Pakhomovsky, Ya.A., 2002. Kovdor. Laplandia minerals, Apatity, Russia. 326 pp.

Kalfoun, F., Ionov, D., Merlet, C., 2002. HFSE residence and Nb/Ta ratios in metasomatized, rutile-bearing mantle peridotites. Earth Planet. Sci. Lett. 199, 49–65.

Kamber, B.S., Collerson, K.D., 2000. Zr/Nb systematics of ocean island basalts reassessed — the case for binary mixing. J. Petrol. 41, 1007–1021.

Kapustin, Yu.L., 1986. Distribution of titanium, niobium and tantalum in rocks and minerals of carbonatite complexes. Transact. USSR Acad. Sci. Earth Sci. Sect. 282, 172–175.

Kempton, P.D., Downes, H., Neymark, L.A., Wartho, J.A., Zartman, R.E., Sharkov, E.V., 2001. Garnet granulite xenoliths from the northern Baltic Shield — the underplated lower crust of a Paleoproterozoic large igneous province? J. Petrol. 42, 731–763.

Kennedy, A.K., Lofgren, G.E., Wasserburg, G.J., 1993. An experimental study of trace element partitioning between olivine, orthopyroxene and melt in chondrules: equilibrium values and kinetic effects. Earth Planet. Sci. Lett. 115, 177–195.

Kirnarskii, Yu.M., Polezhaeva, L.I., 1975. On the content and occurrence mode of Nb and Ta in magnetite from carbonatite complexes. Materials on the mineralogy and geochemistry of alkaline-rock complexes of the Kola Peninsula. Kola Science Center, Apatity, Russia, pp. 203–214 (in Russ.).

Kjarsgaard, B., Peterson, T., 1991. Nephelinite-carbonatite liquid immiscibility at Shombole volcano, East Africa: Petrographic and experimental evidence. Mineral. Petrol. 43, 293–314.

Klemme, S., Meyer, H.-P., 2003. Trace element partitioning between baddeleyite and carbonatite melt at high pressures and high temperatures. Chem. Geol. 199, 233–242.

Klemme, S., van der Laan, S.R., Foley, S.F., Günther, D., 1995. Experimentally determined trace and minor element partitioning between clinopyroxene and carbonatite melt under upper mantle conditions. Earth Planet. Sci. Lett. 133, 439–448.

Kramm, U., Kogarko, L.N., Kononova, V.A., Vartiainen, H., 1993. The Kola Alkaline Province of the CIS and Finland: Precise Rb–Sr ages define 380–360 Ma age range for all magmatism. Lithos 30, 33–44.

Krasnova, N.I., Balaganskaya, E.G., Garcia, D., 2004. Kovdor — classic phoscorites and carbonatites. In: Wall, F., Zaitsev, A.N. (Eds.), Phoscorites and Carbonatites from Mantle to Mine: the Key Example of the Kola Alkaline Province. Mineralogical Society, London, pp. 99–132.

Kravchenko, S.M., Bagdasarov, Yu.A., 1987. Geochemistry, mineralogy and genesis of apatite-bearing massifs (Maimecha-Kotuy carbonatite province). Nauka, Moscow. 129 pp (in Russ.).

Krivovichev, S.V., Armbruster, T., Yakovenchuk, V.N., Pakhomovsky, Ya.A., Men'shikov, Yu.P., 2003. Crystal structures of lamprophyllite-2M and lamprophyllite-2O from the Lovozero alkaline massif, Kola peninsula, Russia. Eur. J. Mineral. 15, 711–718.

Kukharenko, A.A., Orlova, M.P., Bulakh, A.G., Bagdasarov, E.A., Rimskaya-Korsakova, O.M., Nefedov, E.I., Il'inskiy, G.A., Sergeev, A.S., Abakumova, N.B., 1965. The Caledonian complex of ultramafic, alkaline rocks and carbonatites of the Kola Peninsula and northern Karelia. Nedra Press, Moscow. 772 pp (in Russ.).

Lapin, A.V., 1979. Mineral parageneses of apatite ores and carbonatites of the Sebl'yavr Massif. Int. Geol. Rev. 21, 1043–1052.

Lapin, A.V., Vartiainen, H., 1983. Orbicular and spherulitic carbonatites from Sokli and Vuorijärvi. Lithos 16, 53–60.

LaTourrette, T., Hervig, R.L., Holloway, J.R., 1995. Trace element partitioning between amphibole, phlogopite, and basanite melt. Earth Planet. Sci. Lett. 135, 13–30.

Laurora, A., Mazzucchelli, M., Rivalenti, G., Vannucci, R., Zanetti, A., Barbieri, M.A., Cingolani, C.A., 2001. Metasomatism and melting in carbonated peridotite xenoliths from the mantle wedge: the Gobernador Gregores case (Southern Patagonia). J. Petrol. 42, 69–87.

Le Bas, M.J., Keller, J., Kejie, T., Wall, F., Williams, C.T., Peishan, Z., 1992. Carbonatite dykes at Bayan Obo, Inner Mongolia, China. Mineral. Petrol. 46, 195–228.

Lee, W.-J., Wyllie, P.J., 1998a. Petrogenesis of carbonatite magmas from mantle to crust, constrained by the system CaO–(MgO+FeO*)–(Na_2O+K_2O)–($SiO_2+Al_2O_3+TiO_2$)–CO_2. J. Petrol. 39, 495–517.

Lee, W.-J., Wyllie, P.J., 1998b. Processes of crustal carbonatite formation by liquid immiscibility and differentiation, elucidated by model systems. J. Petrol. 39, 2005–2013.

Lee, W.J., Wyllie, P.J., 2000. The system CaO–MgO–SiO_2–CO_2 at 1 GPa, metasomatic wehrlites, and primary carbonatite magmas. Contrib. Mineral. Petrol. 138, 214–228.

Lee, M.J., Garcia, D., Moutte, J., Williams, C.T., Wall, F., 2004. Carbonatites and phoscorites from the Sokli Complex, Finland. In: Wall, F., Zaitsev, A.N. (Eds.), Phoscorites and carbonatites from mantle to mine: the key example of the Kola Alkaline Province. Mineralogical Society, London, pp. 133–162.

Le Roex, A.P., Lanyon, R., 1998. Isotope and trace element geochemistry of Cretaceous Damaraland lamprophyres and carbonatites, northwestern Namibia: evidence for plume-lithosphere interactions. J. Petrol. 39, 1117–1146.

Linnen, R.L., Keppler, H., 2002. Melt composition control of Zr/Hf fractionation in magmatic processes. Geochim. Cosmochim. Acta 66, 3293–3301.

Lundstrom, C.C., Shaw, H.F., Ryerson, F.J., Williams, Q., Gill, J., 1998. Crystal chemical control of clinopyroxene-melt partitioning in the Di–Ab–An system: implications for elemental fractionations in the depleted mantle. Geochim. Cosmochim. Acta 62, 2849–2862.

Macdonald, R., Kjarsgaard, B.A., Skilling, I.P., Davies, G.R., Hamilton, D.L., Black, S., 1993. Liquid immiscibility between trachyte and carbonate in ash flow tuffs from Kenya. Contrib. Mineral. Petrol. 114, 276–287.

Mariano, A., 1989. Nature of economic mineralization in carbonatites and related rocks. In: Bell, K. (Ed.), Carbonatites: genesis and evolution. Unwin Hyman, London, pp. 149–176.

McDonough, W.F., Sun, S.-s., 1995. The composition of the Earth. Chem. Geol. 120, 223–253.

Menzies, M., Chazot, G., 1995. Fluid processes in diamond to spinel facies shallow mantle. J. Geodyn. 20, 387–415.

Moine, B.N., Gregoire, M., O'Reilly, S.Y., Sheppard, S.M.F., Cottin, J.Y., 2001. High field strength element fractionation in the upper mantle: evidence from amphibole-rich composite mantle xenoliths from the Kerguelen Islands (Indian Ocean). J. Petrol. 42, 2145–2167.

Moore, K.R., Wood, B.J., 1998. The transition from carbonate to silicate melts in the CaO–MgO–SiO_2–CO_2 system. J. Petrol. 39, 1943–1951.

Neumann, E.-R., Wulff-Pedersen, E., Pearson, N.J., Spencer, E.A., 2002. Mantle xenoliths from Tenerife (Canary Islands): evidence for reactions between mantle peridotites and silicic carbonatite melts inducing Ca metasomatism. J. Petrol. 43, 825–857.

Nielsen, R.L., Beard, J.S., 2000. Magnetite-melt HFSE partitioning. Chem. Geol. 164, 21–34.

Oberti, R., Ungaretti, L., Cannillo, E., Hawthorne, F.C., 1992. The behaviour of Ti in amphiboles: I. Four- and six-coordinate Ti in richterite. Eur. J. Mineral. 4, 425–439.

Onuma, N., Ninomiya, Sh., Nagasawa, H., 1981. Mineral/groundmass partition coefficients for nepheline, melilite, clinopyroxene and perovskite in melilite–nepheline basalt, Nyiragongo, Zaire. Geochem. J. 15, 221–228.

Peterson, T.D., 1989. Peralkaline nephelinites. I. Comparative petrology of Shombole and Oldoinyo L'engai, East Africa. Contrib. Mineral. Petrol. 101, 458–478.

Petibon, C.M., Jenner, G.A., Kjarsgaard, B.A., 1998. The genesis of natrocarbonatites: constraints from experimental petrology and trace element partition coefficients. Mineral. Mag. 62A, 1161–1162.

Plá Cid, J., Nardi, L.V.S., Gisbert, P.E., Merlet, C., Boyer, B., 2005. SIMS analyses on trace and rare earth elements in coexisting clinopyroxene and mica from minette mafic enclaves in potassic syenites crystallized under high pressure. Contrib. Mineral. Petrol. 148, 675–688.

Powell, W., Zhang, M., O'Reilly, S.Y., Tiepolo, M., 2004. Mantle amphibole trace-element and isotopic signatures trace multiple metasomatic episodes in lithospheric mantle, western Victoria, Australia. Lithos 75, 141–171.

Pozharitskaya, L.K., Samoylov, V.S., 1972. Petrology, mineralogy and geochemistry of the carbonatites of East Siberia. Nauka, Moscow, Russia. 268 pp (in Russ.).

Prowatke, S., Klemme, S., 2005. Effect of melt composition on the partitioning of trace elements between titanite and silicate melt. Geochim. Cosmochim. Acta 69, 695–709.

Samoylov, V.S., 1984. Geochemistry of carbonatites. Nauka Press, Moscow (in Russ.).

Scordari, F., Schingaro, E., Pedrazzi, G., 1999. Crystal chemistry of melanites from Mt. Vulture (Southern Italy). Eur. J. Mineral. 11, 855–869.

Sinclair, W., Eggleton, R.A., 1982. Structure refinement of zirkelite from Kaiserstuhl, West Germany. Am. Mineral. 67, 615–620.

Sinclair, W., Eggleton, R.A., McLaughlin, G.M., 1986. Structure refinement of calzirtite from Jacupiranga, Brazil. Am. Mineral. 71, 815–818.

Sindern, S., Zaitsev, A.N., Demeny, A., Bell, K., Chakhmouradian, A.R., Kramm, U., Moutte, J., Rukhlov, A.S., 2004. Mineralogy and geochemistry of silicate dyke rocks associated with carbonatites from the Khibina complex (Kola, Russia) — isotope constraints on genesis and small-scale mantle sources. Mineral. Petrol. 80, 215–239.

Schmidt, K.H., Botazzi, P., Vanucci, R., Mengel, K., 1999. Trace element partitioning between phlogopite, clinopyroxene and leucite lamproite melt. Earth Planet. Sci. Lett. 168, 287–299.

Skulski, T., Minarik, W., Watson, E.B., 1994. High-pressure experimental trace-element partitioning between clinopyroxene and basaltic melts. Chem. Geol. 117, 127–147.

Späth, A., Le Roex, A.P., Opiyo-Akech, N., 2001. Plume-lithosphere interaction and the origin of continental rift-related alkaline volcanism — the Chyulu Hills Volcanic Province, southern Kenya. J. Petrol. 42, 765–787.

Subbotin, V.V., Subbotina, G.F., 2000. Minerals of the pyrochlore group in phoscorites and carbonatites of the Kola Peninsula. Vest. Murmansk. Gosudarst. Techn. Univ., vol. 3, pp. 273–284 (in Russ.).

Suk, N.I., 2001. Experimental study of liquid immiscibility in silicate–carbonate systems. Petrology 9, 477–487.

Sweeney, R.J., 1994. Carbonatite melt compositions in the Earth's mantle. Earth Planet. Sci. Lett. 128, 259–270.

Sweeney, R.J., Green, D.H., Sie, S.H., 1992. Trace and minor element partitioning between garnet and amphibole and carbonatitic melt. Earth Planet. Sci. Lett. 113, 1–14.

Sweeney, R.J., Prozesky, V., Przybylowicz, W., 1995. Selected trace and minor element partitioning between peridotite minerals and carbonatite melts at 18–46 kbar pressure. Geochim. Cosmochim. Acta 59, 3671–3683.

Thompson, G.M., Malpas, J., 2000. Mineral/melt partition coefficients of oceanic alkali basalts determined on natural samples using laser ablation-inductively coupled plasma-mass spectrometry (LAM-ICP-MS). Mineral. Mag. 64, 85–94.

Tiepolo, M., Bottazzi, P., Foley, S.F., Oberti, R., Vannucci, R., Zanetti, A., 2001. Fractionation of Nb and Ta from Zr and Hf at mantle depths: the role of titanian pargasite and kaersutite. J. Petrol. 42, 221–232.

Tolstikhin, I.N., Kamensky, I.L., Marty, B., Nivin, V.A., Vetrin, V.R., Balaganskaya, E.G., Ikorsky, S.V., Gannibal, M.A., Weiss, D., Verhulst, A., Demaiffe, D., 2002. Rare gas isotopes and parent trace elements in ultrabasic-alkaline–carbonatite complexes, Kola Peninsula: identification of lower mantle plume component. Geochim. Cosmochim. Acta 66, 881–901.

Veksler, I.V., Petibon, C., Jenner, G.A., Dorfman, A.M., Dingwell, D.B., 1998a. Trace element partitioning in immiscible silicate-carbonate liquid systems: an initial experimental study using a centrifuge autoclave. J. Petrol. 39, 2095–2104.

Veksler, I.V., Nielsen, T.F.D., Sokolov, S.V., 1998b. Mineralogy of crystallized melt inclusions from Gardiner and Kovdor ultramafic alkaline complexes: implications for carbonatite genesis. J. Petrol. 39, 2015–2031.

Verhulst, A., Balaganskaya, E., Kirnarsky, Y., Demaiffe, D., 2000. Petrological and geochemical (trace elements and Sr–Nd isotopes) characteristics of the Paleozoic Kovdor ultramafic, alkaline and carbonatite intrusion (Kola Peninsula, NW Russia). Lithos 51, 1–25.

Vetrin, V.R., Kamensky, I.L., Ikorsky, S.V., 2003. Age of mantle metasomatism and formation of the Kola Paleozoic Alkaline Province. Dokl. Earth Sci. 389, 212–215.

Viladkar, S.G., Wimmenauer, W., 1986. Mineralogy and geochemistry of the Newania carbonatite–fenite complex, Rajasthan, India. Neues Jahrb. Mineral. Abh. 156, 1–21.

Vorob'ev, E.I., 2000. Book review. Geol. Geofiz. 41, 1821–1823 (in Russ.).

Wall, F., Zaitsev, A.N. (Eds.), 2004. Phoscorites and carbonatites from mantle to mine: the key example of the Kola Alkaline Province. Mineral. Soc., London. 498 pp.

Wallace, M., Green, D.H., 1988. An experimental determination of primary carbonatite composition. Nature 335, 343–346.

Wedepohl, K.H., 1995. The composition of the continental crust. Geochim. Cosmochim. Acta 59, 1217–1232.

Williams, C.T., 1996. The occurrence of niobian zirconolite, pyrochlore and baddeleyite in the Kovdor carbonatite complex. Mineral. Mag. 60, 639–646.

Woolley, A.R., Kempe, D.R.C., 1989. Carbonatites: nomenclature, average chemical compositions, and element distribution. In: Bell, K. (Ed.), Carbonatites: genesis and evolution. Unwin Hyman, London, pp. 1–14.

Wyllie, P.J., Lee, W.-J., 1998. Model system controls on conditions for formation of magnesiocarbonatite and calciocarbonatite magmas from the mantle. J. Petrol. 39, 1885–1893.

Yamada, T., Mizuno, M., Ishizuka, T., Noguchi, T., 1988. Liquidus-curve measurement in the system zirconia–hafnia. Science and technology of zirconia III. Adv. Ceram. 24, 959–964.

Yaxley, G.M., Green, D.H., 1996. Experimental reconstruction of sodic dolomitic carbonatite melts from metasomatised lithosphere. Contrib. Mineral. Petrol. 124, 359–369.

Yaxley, G.M., Kamenetsky, V., 1999. In situ origin for glass in mantle xenoliths from southeastern Australia: insights from trace element compositions of glasses and metasomatic phases. Earth Planet. Sci. Lett. 172, 97–109.

Yaxley, G.M., Green, D.H., Kamenetsky, V., 1998. Carbonatite metasomatism in the southeastern Australian lithosphere. J. Petrol. 39, 1917–1930.

Zaitsev, A.N., Sitnikova, M.A., Subbotin, V.V., Fernández-Suárez, J., Jeffries, T.E., 2004. Sallanlatvi complex — a rare example of magnesite and siderite carbonatites. In: Wall, F., Zaitsev, A.N. (Eds.), Phoscorites and carbonatites from mantle to mine: the key example of the Kola Alkaline Province. Mineralogical Society, London, pp. 201–245.

Zaitsev, A. N., Keller, J., in press. Mineralogical and chemical transformation of Oldoinyo Lengai natrocarbonatites, Tanzania. Lithos.

Zanetti, A., Tiepolo, M., Oberti, R., Vannucci, R., 2004. Trace-element partitioning in olivine: modeling of a complete data set from a synthetic hydrous basanite melt. Lithos 75, 39–54.